Available online at www.sciencedirect.com
ScienceDirect
Mitochondrion 7 (2007) 125–132
Mitochondrion
www.elsevier.com/locate/mito

Mitochondria and apicoplast of *Plasmodium falciparum*: Behaviour on subcellular fractionation and the implication

Tamaki Kobayashi [a], Shigeharu Sato [b], Shinzaburo Takamiya [c], Kanako Komaki-Yasuda [d], Kazuhiko Yano [d], Ayami Hirata [e], Izumi Onitsuka [e], Masayuki Hata [a], Fumika Mi-ichi [a], Takeshi Tanaka [a], Toshiharu Hase [f], Atsushi Miyajima [e], Shin-ichiro Kawazu [d], Yoh-ichi Watanabe [a], Kiyoshi Kita [a,*]

[a] *Department of Biomedical Chemistry, Graduate School of Medicine, The University of Tokyo, 7-3-1 Hongo, Buinkyo-ku, Tokyo 113-0033, Japan*
[b] *Division of Parasitology, National Institute for Medical Research, The Ridgeway, Mill Hill, London NW7 1AA, UK*
[c] *Department of Molecular and Cellular Parasitology, Juntendo University School of Medicine, 2-1-1 Hongo, Bunkyo-ku, Tokyo 113-8421, Japan*
[d] *Research Institute, International Medical Center of Japan, 1-21-1 Toyama, Shinjuku-ku, Tokyo 162-8655, Japan*
[e] *Laboratory of Cell Growth and Differentiation, Institute of Molecular and Cellular Biosciences, The University of Tokyo, 1-1-1 Yayoi, Bunkyo-ku, Tokyo 113-0032, Japan*
[f] *Division of Enzymology, Institute for Protein Research, Osaka University, 3-2 Yamadaoka, Suita, Osaka 565-0871, Japan*

Received 19 April 2006; accepted 21 September 2006
Available online 9 December 2006

Abstract

The mitochondrion and the apicoplast of the malaria parasite, *Plasmodium* spp. is microscopically observed in a close proximity to each other. In this study, we tested the suitability of two different separation techniques – Percoll density gradient centrifugation and fluorescence-activated organelle sorting – for improving the purity of mitochondria isolated from the crude organelle preparation of *Plasmodium falciparum*. To our surprise, the apicoplast was inseparable from the plasmodial mitochondrion by each method. This implies these two plasmodial organelles are bound each other. This is the first experimental evidence of a physical binding between the two organelles in *Plasmodium*.

Keywords: *Plasmodium falciparum*; Mitochondrion; Apicoplast; Fluorescence-activated organelle fractionation

1. Introduction

Malaria, by far the most important tropical parasitic disease, is caused by a group of parasites *Plasmodium* spp. belonging to the phylum Apicomplexa. Currently, various anti-malarial drug resistant parasite strains are reported and there is a long way for the development of vaccine. Emergence of insecticide resistant mosquito vector limits the current control schemes as well (Greenwood et al., 2005). In order to control this world problem, studies seeking for unique properties of the parasite are indispensable.

Previous study reported malaria parasites obtain most of their energy from glycolysis, if not all (Roth et al., 1988) and malaria parasite possesses one mitochondrion with various shapes at different stages of the intra-erythrocytic development and it is acristae (Slomianny and Prensier, 1986). Mitochondria of *Plasmodium* species carries 6-kb genome, which is the smallest mitochondrial genome ever been reported and encoding only 3 open reading frames with homology to classical mitochondrial protein, cytochrome *c* oxidase subunit I, cytochrome *c* oxidase subunit III and cytochrome *b*, as well as abbreviated rRNA genes (Vaidya et al., 1989; Feagin, 1992). Thus this

Abbreviations: DHOD, dihydroorotate dehydrogenase; FOS, fluorescence-activated organelle sorting; RBC, red blood cell.

* Corresponding author. Tel.: +81 3 5841 3526; fax: +81 3 5841 3444.
E-mail address: kitak@m.u-tokyo.ac.jp (K. Kita).

1567-7249/$ - see front matter © 2006 Elsevier B.V. and Mitochondria Research Society. All rights reserved.
doi:10.1016/j.mito.2006.11.021

organelle heavily depends on most of the proteins and all tRNAs supplied from the outside.

Biochemical analysis suggested that *Plasmodium falciparum* might lack TCA cycle in the erythrocytic stage (see the review by Sherman, 1979). Recent completion of malaria genome project has revealed that the genes necessary for a complete TCA cycle were present in *P. falciparum* (Gardner et al., 2002). However, it still remains unclear whether the TCA cycle is responsible for the further oxidation of glycolysis product. Nevertheless, the activity of the electron transport chain and the membrane potential of this organelle are indispensable for the survival of the parasite. For example, dihydroorotate dehydrogenase (DHOD) involved in the parasite's *de novo* biosynthesis of pyrimidine requires the functional electron transport chain on the mitochondrial membrane as the electron disposal sink (Gutteridge and Trigg, 1970; Gero et al., 1984; Prapunwattana et al., 1988). More recent study showed that the membrane potential of mitochondria formed by respiration is essential for parasite growth (Srivastava et al., 1999) and complex III (ubiquinol-cytochrome *c* reductase) inhibitor, atovaqone, an anti-malarial that is currently in use is reported to disrupt mitochondrial membrane potential resulting in parasite growth reduction (Srivastava et al., 1997).

Aikawa (1966) carried out an extensive morphological study by electron microscope and found a distinctive organelle in the cell of the malaria parasite. This organelle is multi-membrane bound, always observed adjacent to the mitochondrion (see the review by Bannister et al., 2000). Later, a non-mitochondrial extra-chromosomal DNA encoding a set of genes characteristic of the plastid genome was found in apicomplexan parasites including *Plasmodium* spp. *Toxoplasma gondii* and *Theileria* spp. (Wilson et al., 1996; Kohler et al., 1997) localized the plastid genome-like DNA to the multi-membrane organelle in *T. gondii* by *in situ* hybridization, revealing that the distinctive multi-membrane organelle is the plastid of the apicomplexan parasite. The apicomplexan plastid, which is non-photosynthetic, is often called "the apicoplast" for abbreviation. The genome of the apicoplast is one of the smallest known plastid genomes (Wilson et al., 1996; Gardner et al., 2005). The apicoplast depends heavily on proteins imported post-translationally from the cytosol (see the review by Ralph et al., 2004), as does the mitochondrion.

For biochemical studies of each organelle of *Plasmodium* spp., it is necessary to obtain the pure sample. Fry and Beesley (1991) reported a method to prepare the mitochondria from *Plasmodium* spp. by Percoll density gradient centrifugation. Takashima et al. (2001) reported another preparation method using nitrogen cavitation. The mitochondrial preparation by the latter method exhibited a significantly higher succinate dehydrogenase activity than that by the former method (Takashima et al., 2001). By contrast, no method for preparing the plasmodial apicoplast with a significant purity has been reported.

In this study, we combined nitrogen cavitation method with two different fractionation methods, Percoll density gradient centrifugation or fluorescence-activated organelle sorting (FOS), to prepare the mitochondrion of higher purity from *P. falciparum*. Surprisingly, we found that the mitochondrion and the apicoplast were recovered in the same fraction by each fractionation methods, most likely because the two organelles are bound each other. To our knowledge, this is the first report that suggests the presence of a physical connection between the mitochondrion and the apicoplast of *P. falciparum*.

2. Materials and methods

2.1. Parasite cultivation and handling

Plasmodium falciparum (Honduras-1 strain and 3D7 strain) was cultured following the method reported by Trager and Jensen (1976) with modifications. The culture was maintained with 3% hematocrit type A human red blood cell (RBC) in RPMI 1640 medium (Invitrogen) supplemented with 10% (v/v) type A human serum. Prior to the preparation of crude mitochondrial fraction, parasites were synchronised by 5% (w/v) sorbitol as it was described previously (Lambros and Vanderberg, 1979).

2.2. Preparation of the crude *P. falciparum* mitochondria fraction

Plasmodium falciparum-infected RBC were collected by centrifugation at 800*g* for 10 min at 4 °C (LX-120, TOMY) when parasitemia is more than 5% but not exceeding 10%. Parasite was mainly trophozoite stage as it was confirmed by observing the Giemsa's stained smear. Trophozoite stage was considered because DHOD-specific activity is the highest (F. Mi-ichi, Personal communication). The crude *P. falciparum* were disrupted by nitrogen cavitation as described (Takashima et al., 2001). The pellet obtained after the centrifugation at 23,000*g* for 20 min at 4 °C (Himac CR22, HITACHI) was suspended in 200–400 μl MSE buffer (225 mM mannitol, 75 mM sucrose, 0.1 mM EDTA (Dojin), 3 mM Tris–HCl; pH 7.4) and characterized as a crude mitochondrial fraction (Fig. 1).

2.3. Subcellular fractionation of *P. falciparum* mitochondria with the Percoll density gradient centrifugation

The crude mitochondrial fraction prepared from *P. falciparum* Honduras-1 strain (1.5 mg protein) was brought to a total volume of 8 ml in 23% (v/v) Percoll (GE Healthcare) in MSE. Percoll sample was centrifuged at 100,000*g* for 1 h at 4 °C (Himac SCP70H, HITACHI, rotor No. RP40). Together with the mitochondrial fraction, beads marker provided by the manufacture was centrifuged in parallel to confirm the formation of gradient and density of each fraction. The gradient was fractionated from top to bottom with glass Pasteur pipette (400 μl/ fraction). The formation

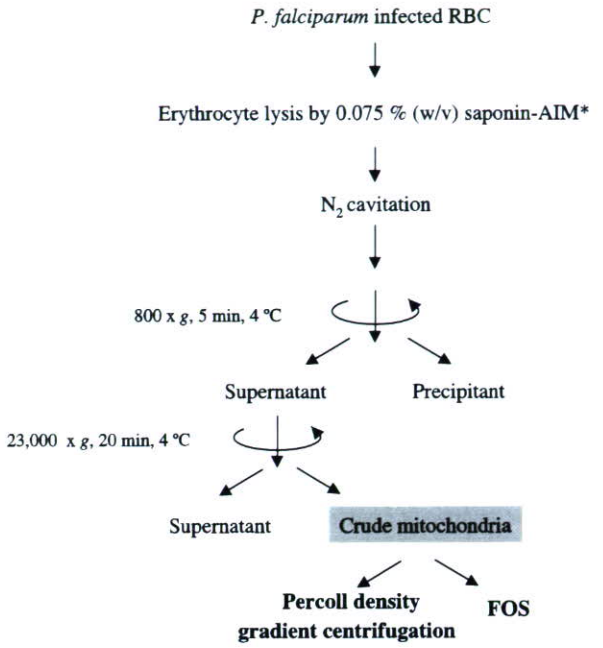

Fig. 1. Crude mitochondria preparation from *P. falciparum* *AIM (120 mM KCl, 20 mM NaCl, 10 mM Pipes, 1 mM $MgCl_2$, 5 mM glucose; pH 6.7).

of the gradient can be affected by factors such as the angle of the rotor. Therefore, it is critical to monitor the formation of the desired gradient by using the density marker beads all the time when one uses different centrifuge and rotor.

DHOD activity was measured to determine the fraction containing mitochondria (Mi-Ichi et al., 2005). DHOD assay was performed at 25 °C using UV3000 spectrophotometer (SHIMADZU) with 1 ml of the reaction mixture containing 45 μM 2,6-dichlorophenolindophenol (DCIP) (Sigma), 100 μM ubiquinone-2 (Sigma) and 2 mM KCN in 30 mM Tris–HCl (pH 8.0). The reaction was initiated by adding 500 μM dihydroorotate and the production of reduced DCIP was monitored at 600 nm (ε=21 mM^{-1} cm^{-1}).

2.4. Protein assay

Protein concentration of *P. falciparum* sample was determined by Bradford method (Bradford, 1976) using Bio-Rad protein assay reagent according to the manual provided by the manufacturer, with bovine serum albumin (PIERCE) as a standard. For the sample that contains Percoll, Percoll was precipitated under the presence of 250 mM NaOH and 0.025% (w/v) Triton X-100 as it was reported (Vincent and Nadeau, 1983) prior to the protein assay.

2.5. Western blot analysis

As Percoll interferes with SDS–PAGE, the fraction of interest was diluted with MSE buffer up to 8.5 ml and centrifuged at 220,000*g* for 1 h at 4 °C (CP10α, 70H, HITACHI) to remove Percoll. Samples were collected as floating pellet and suspended in MSE up to 1.5 ml. Suspended pellet was transferred to 1.5 ml tube and centrifuged at 20,000*g* for 10 minutes at 4 °C (TOMY MX-160). The pellet was re-suspended in MSE buffer. Prepared samples were then run on 12.5% polyacrylamide gel and transferred to nitrocellulose membrane. Membranes were blocked with 5% (w/v) non-fat skim milk powder in 0.5% (v/v) Tween–Tris-buffered saline and afterwards probed with polyclonal antibodies specific to mitochondrion or apicoplast. For the detection of mitochondrion and apicoplast, serum against recombinant *P. falciparum* iron–sulfur cluster subunit of complex II (rPfIp) and ferredoxin (rPfFd) were raised in mouse and rabbit, respectively. The dilution for the first antibody was 1:2000 for anti-rPfIp serum and 1:1000 for anti-rPfFd serum.

2.6. Electron microscopic observation of the subcellular-fractionated sample by the Percoll density gradient centrifugation

Percoll was removed from the sample as described above. Obtained pellet was suspended in fixative solution containing 2% (v/v) glutaraldehyde in 20 mM sodium phosphate buffer (pH 6.8): MSE buffer = 1:1. The sample was fixed overnight at 4 °C and subsequently washed with 20 mM Sodium phosphate buffer (pH 6.8): MSE buffer = 1:1 for three times. The fixed sample was then dehydrated and embedded in resin. Serial sections were cut and observed by transmission electron microscope (HITACHI H-7100).

2.7. GFP fusion constructs and P. falciparum transfection

The expression vector, pSSPF2/PfHSP60-GFP (Sato et al., 2003) was transfected to *Escherichia coli* DH5α and the transfected *E. coli* was grown in the terrific broth. Plasmids were collected by centrifugation and was purified using Plasmid Maxi Kit (Qiagen). The plasmid was verified with restriction digestion using *Bgl*II and *Xho*I, followed by agarose gel electrophoresis.

The transfection of *P. falciparum* 3D7 was done following the previous report (Sato et al., 2003) with slight modifications. 100 μl infected RBC at approximately 10% ring stage parasitemia was suspended in three volumes of cytomix (van den Hoff et al., 1992) containing 50 μg of plasmid DNA. Total 400 μl of the RBC suspension was electroporated in a 0.2 cm cuvette using Gene Pulser II (Bio-Rad) (0.31 kV, 975 μF). After the transfection, parasites were maintained in the medium supplemented with 5 nM WR99210 as it was described previously (Sato et al., 2003).

2.8. Immunofluorescent studies

Infected erythrocytes and mitochondrial fraction was observed using confocal microscope LSM510 (Zeiss).

Parasites expressing fluorescent protein were incubated for 30 min at 37 °C with MitoTracker Red CM-H_2XRos (Molecular Probes) diluted to 100 nM in culture medium. After the incubation, the culture was once washed with culture medium or AIM medium before microscopy observation.

2.9. Flow cytometry analysis and organelle sorting of transfected parasites

Plasmodium falciparum 3D7 strain expressing GFP was homogenized by nitrogen cavitation method and the crude mitochondrial fraction was prepared according to the procedure described in the previous section. The prepared mitochondrial fraction was analyzed and sorted by EPICS ALTRA (Beckman Coulter). The size of the sorted particles was determined by Flow Cytometry Size calibration Kit (Molecular Probes). Sorted sample were centrifuged and the precipitant was suspended with MSE.

2.10. Detection of organelle by PCR

The primer set to detect apicoplast genome was for the large subunit of rRNA gene, 5′-GAC CTG CAT GAA AGA TG-3′ and 5′-GTA TCG CTT TAA TAG GCG-3′ as it was described previously (Tan et al., 1997). The primer set to detect mitochondria genome was for the subunit I of Complex IV (cytochrome *c* oxidase), 5′-GAC CCA ACA TTT GCA GGA GAT C-3′ and 5′-CAT CAA TGG CAG CAT TAC CTA A-3′. The reaction mixture was prepared with 1 μl of the above mentioned sorted sample (out of final volume 100 μl) or diluted crude mitochondrial fraction, 1× PCR buffer (20 mM Tris–HCl (pH 8.4), 50 mM KCl), 1.25 U *Taq* DNA polymerase (Invitrogen), 1.5 mM $MgCl_2$, 200 μM dNTP and 0.25 μM of each primer in a final volume of 50 μl. The volume of samples was determined not to reach the saturation after the PCR cycle.

The PCR was carried out using the following conditions: pre-heating at 95 °C, 3 min; denaturation at 95 °C, 30 s; annealing at 50 °C, 30 s; elongation at 72 °C, 1 min for 30 cycles followed by incubation at 72 °C for 10 min after the final cycle. For the amplification of mitochondrial genome and apicoplast genome, TEMP CONTROL PC-700 (ASTEC) and GeneAmp® PCR system 9700 (Perkin-Elmer) was used, respectively. Amplified products were then analyzed on a 1% (w/v) agarose gel.

In the experimental procedure, chemicals used were a special grade and were purchased from Wako unless otherwise stated.

3. Results

3.1. The mitochondria and apicoplast co-fractionated by the Percoll density gradient centrifugation

Previously, Fry and Beesley (1991) reported a method to prepare plasmodial mitochondria using a density gradient in 22% (v/v) Percoll formed by centrifugation at 10,000*g* for 5 min. As this method has been successfully used in other laboratories (Wilson et al., 1992; Krungkrai, 1995; Krungkrai et al., 1997), we preliminarily tested if this method is directly applicable to improve the purity of mitochondria prepared by nitrogen cavitation method, which showed higher enzyme activities of mitochondria than those of previous method (Takashima et al., 2001).

We found method reported by Fry and Beesley (1991) is not sufficient to separate mitochondria as g-force was too low and the time was too short (data not shown). Thus, we examined different conditions of Percoll density gradient centrifugation that might improve the current mitochondria sample. To estimate the purity of the obtained mitochondria, activity of mitochondria-specific enzyme, dihydroorotate dehydrogenase (DHOD), which is localized in the inner membrane of the mitochondria was measured. The increase in DHOD-specific activity indicates the enrichment of mitochondria.

We optimized the condition to be 23% (v/v) Percoll centrifuged at 100,000*g* for 1 h at 4 °C using Honduras-1 strain. The gradient was confirmed by the control marker beads in each experiment as it is shown in Fig. 2A. After the Percoll density gradient centrifugation of crude mitochondria sample, prominent brown float and dark brown precipitant were observed (Fig. 2A). The density gradient sample was fractionated and recovery profile of the total DHOD activity after the gradient centrifugation showed two peaks (Fig. 2B). The first peak (fractions 8–10) was sharp and more than twice as high total activity as the broad second peak (fractions 12–16). However, owing to the high amount of proteins recovered, the specific activity in the first peak was not improved. By contrast, the second peak of the total activity showed a significantly higher specific activity; the value of fraction 13 (66.2 ± 27.7 nmol/min/mg protein ($n = 3$)) was about 5 times higher than that of the initial sample (12.4 ± 3.01 nmol/min/mg protein ($n = 3$)). Same results were obtained when the fractionations were performed using 3D7 strain.

To assess the degree of contamination of other cell components, the fractions obtained by the Percoll density gradient centrifugation were analysed by electron microscopy. Fractions 13 and 14, which exhibited the highest DHOD-specific activity, contained a number of mitochondria with double membrane (Fig. 3C and D). Interestingly, another type of multi-membrane-bound organelle was also observed adjacent to the mitochondrion (Fig. 3D). A number of hemozoin particles were found in the crude mitochondria preparation before Percoll density gradient centrifugation (Fig. 3A). Fractions 13 and 14 was virtually free from hemozoin particle (Fig. 3B), although other fractions were prevailed by those bodies (Fig. 3E–G). This suggests that the food vacuole was successfully separated from the mitochondrion by the density gradient centrifugation in 23% (v/v) Percoll.

Since the multi-membrane-bound organelle observed adjacent to the mitochondrion seemed to be the apicoplast,

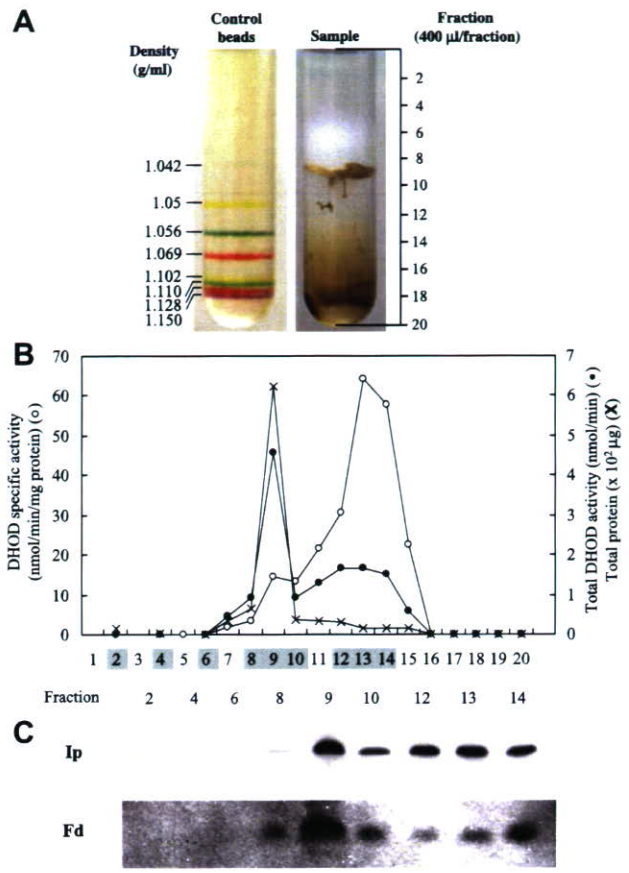

Fig. 2. Percoll density gradient centrifugation. (A) The formation of the gradient was confirmed by beads marker and the density of the control beads were indicated. *P. falciparum* crude mitochondrial fraction was applied to the Percoll density centrifugation forming the brown float and tight brown precipitant. The sample was fractionated from the top to the bottom as indicated. (B) The profile of total protein, DHOD-specific activity and total activity in each fraction of the 23% (v/v) Percoll density gradient centrifugation. The *x*-axis indicates the fraction number and those highlighted were analyzed by the Western blotting. The approximate location of each fraction is briefly indicated in (A). Total protein (X) DHOD total activity (●) and DHOD-specific activity (○). (C) The Western blot analysis of 23% (v/v) Percoll density centrifugation fractions. The localization of mitochondria and apicoplast were determined by using the specific antibodies. Antibody for mitochondria was for succinate dehydrogenase iron–sulfur cluster subunit (Ip) and antibody for apicoplast was for ferredoxin (Fd). eighty microliters of Percoll density fractionation sample was applied each lane.

we probed the fractions made after 23% (v/v) Percoll density gradient centrifugation with the antibody raised against a protein specifically localizing the mitochondrion or the apicoplast. As shown in Fig. 2C, the distribution profile of ferredoxin (Fd), an apicoplast-localizing protein (Vollmer et al., 2001), overlaps that of the iron-sulfer cluster subunit (Ip) of complex II (succinate-ubiquinone reductase), a mitochondrial integral membrane protein (Takeo et al., 2000). This implies even our improved Percoll density gradient centrifugation is not able to separate the mitochondrion from the apicoplast, although it is enough effective to remove the food vacuole or hemozoin particles.

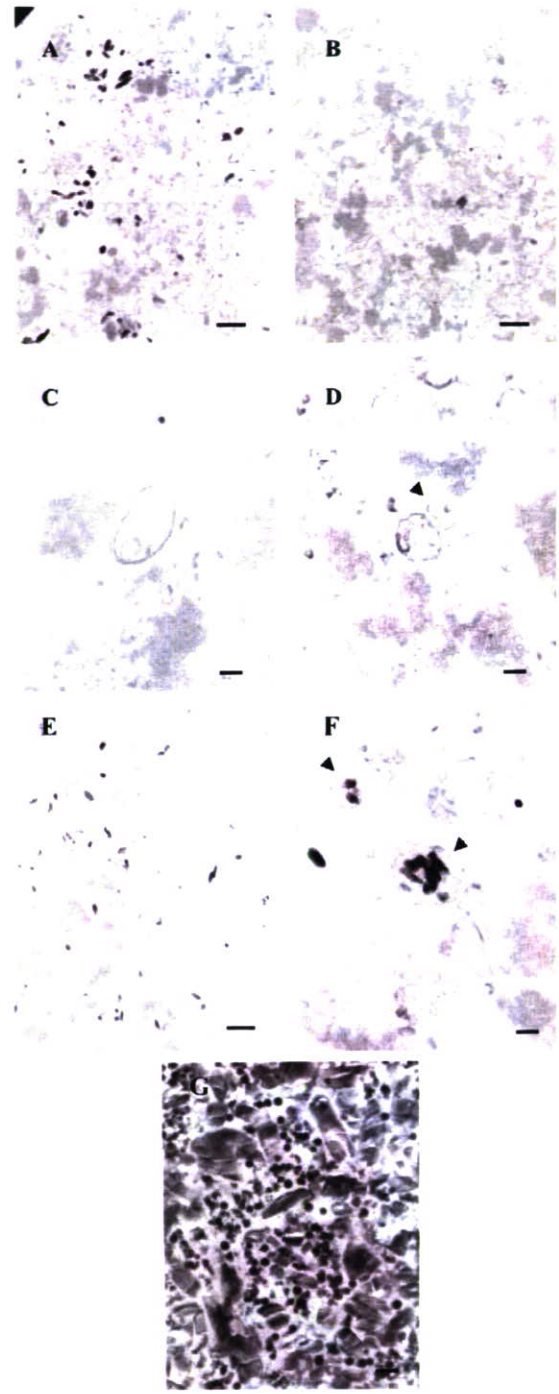

Fig. 3. Electron microscope observation (A) is the crude mitochondria fraction and (B) is the pooled peak fraction of DHOD-specific activity from fraction 13, and 14 after the Percoll density centrifugation (8000×). The dark particles in (A) are significantly reduced in (B), after the Percoll density gradient centrifugation. (C and D) Are observation of the peak DHOD-specific activity at the higher magnification (C; 30,000× and D; 15,000×). The double membrane-bound and multi-membrane-bound structures are indicated by arrows. (E and F) Are the observation of the brown float (fraction 9) at 8000× and 30,000×, respectively. Hemozoin contained in the membrane was observed and from its structure, it is concluded to be a food vacuole. (G) is the tight pellet and the characteristic structure shows it is hemozoin (30,000×). Scale bar; 1 µm for 8000×, 500 nm for 15,000× and 200 nm for 30,000× magnification.

3.2. The mitochondrion and apicoplast are physically bound to each other; co-fractionation of mitochondrion and apicoplast after the fluorescent-activated organelle sorting

As it was found that Percoll density gradient centrifugation is not suitable to remove the apicoplast from the mitochondrion, next we tested another separation technique based on a different physical property of the organelle to recover the apicoplast-free mitochondria from the crude mitochondrial sample.

Plasmodium falciparum 3D7 strain was transfected with a expression plasmid carrying a gene for a GFP derivative that localizes to the mitochondrion (Sato et al., 2003). Specific localization of GFP to the mitochondrion was confirmed by confocal microscope (data not shown) Then, the transfectant and non-transfectant parasites were disrupted by the nitrogen cavitation method and crude mitochondria sample was prepared as it is described in the material and method (Fig. 1). The expression of GFP in mitochondria did not affect the specific activity of mitochondria marker enzyme and therefore the property of mitochondria was not changed at least at the level of electron transfer. In addition, the particle size of the crude mitochondrial sample from GFP-expressing and non-GFP-expressing was not altered depending on the expression of GFP (Fig. 4, inserted figures).

The crude mitochondria fractions prepared from GFP expressing and non-GFP expressing *P. falciparum* was analyzed by flow cytometry. The crude mitochondria preparation from the GFP-expressing transfectant emitted significantly higher fluorescence compared to that of non-transfectant control (Fig. 4A and B). We recovered GFP-positive sample after the fluorescence-activated organelle sorting (FOS) and performed PCR to detect the presence of mitochondria using a specific primers for subunit I of cytochrome *c* oxidase, which is encoded on the mitochondrial DNA. Both the crude sample before FOS and the GFP positive fraction recovered after FOS gave a clear band, confirming the presence of the mitochondrial genomic DNA in these samples (Fig. 5, lanes 1 and 3). In addition, PCR product from apicoplast genomic DNA, large subunit of ribosomal RNA, were also detected (Fig. 5, lanes 2 and 4). This result implies that apicoplast were sorted together with mitochondria by FOS.

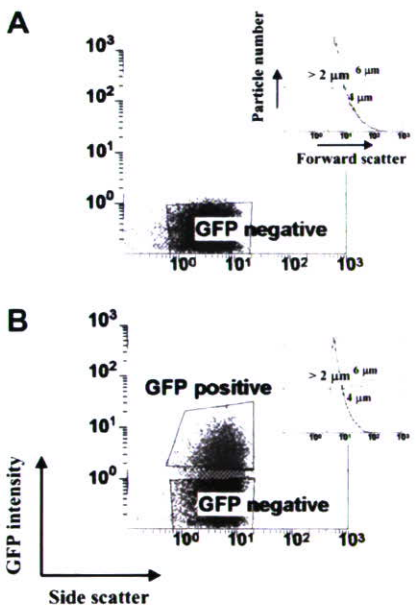

Fig. 4. FOS analysis of crude mitochondria fraction; control and GFP expressing sample. (A) The flow cytometry analysis of the crude mitochondrial fraction from control *P. falciparum* 3D7. The square "GFP negative" indicates the background. (B) The crude mitochondrial fraction prepared from GFP expressing transfectant. The size was determined by the calibration beads. The fraction of the sample expressing significantly high GFP signal were sorted as "GFP positive". The inserted figures show the particle size of the applied crude mitochondria sample.

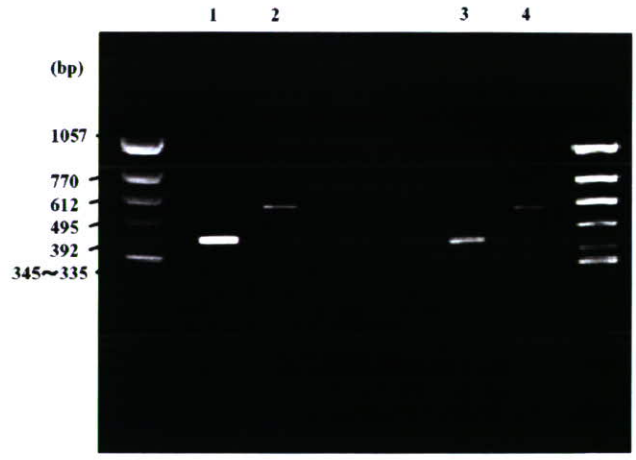

Fig. 5. PCR analysis of mitochondrial fraction and FACS sample. Lanes 1 and 2; crude mitochondria sample. Lane 1 is mitochondria genome-specific primer set and lane 2 is apicoplast genome-specific primer set. Lanes 3 and 4; after the organelle sorting. Lane 3 is mitochondria genome-specific primer set and lane 4 is apicoplast genome-specific primer set. For the detection of mitochondria, the primer set to amplify a part of gene encoding subunit I of cytochrome *c* oxidase was used. For the detection of apicoplast, a part of gene encoding large subunit of ribosomal RNA was used.

4. Discussion

The biochemical study of plasmodial mitochondria has been limited due to the difficulty to prepare sample with high quality and quantity. Previously we have reported the improved mitochondrial preparation from *P. falciparum* using nitrogen cavitation method (Takashima et al., 2001). In this study, we investigated the method to obtain a mitochondrial preparation of better quality by combining nitrogen cavitation with another fractionation method.

Percoll density gradient centrifugation is a well known method to prepare mitochondrial fraction from various organisms including *P. falciparum* and *Plasmodium yoelii* (Fry and Beesley, 1991). The method also has been used for the subcellular fractionation and purification of

mitochondrial enzymes from *Plasmodium* (Krungkrai, 1995, 1997). However, we have found that the purity of the mitochondrial sample prepared by the nitrogen cavitation method could not be improved by the method Fry and Beesley reported (1991). Instead, longer centrifugation with stronger force resulted in a better separation of the mitochondrion (23% (v/v) Percoll, 100,000*g* for 1 h). It is probably because each subcellular structure in the cell was less damaged by nitrogen cavitation in our method than the homogenization with glass-Teflon homogenizer by Fry and Beesley (1991). Indeed, the intact food vacuole containing haemozoin crystals was observed even after our fractionation method (Fig. 3F), and we previously noted that the mitochondrial activity represented by the succinate dehydrogenase was 2 to 3 times higher in of the crude mitochondrial preparation prepared by nitrogen cavitation (Takashima et al., 2001) than those prepared by other conventional methods (Suraveratum et al., 2000).

In this study, the DHOD-specific activity increased about 5 times after the Percoll density gradient centrifugation in the second peak (Fig. 2B), indicating that the contaminants were removed. Indeed, the observation by the electron microscope showed that hemozoin and food vacuole were significantly reduced after the Percoll density gradient centrifugation. Electron microscopic analysis confirmed that the mitochondrion with double membrane was enriched in the fractions forming the second peak (Fig. 3C and D).

Unlike the food vacuole, the apicoplast was not separated from the mitochondrion after the Percoll density gradient centrifugation. It might be because the organelle, by chance, shares the similar density with the mitochondrion. We examined this possibility by a different fractionation method – fluorescence-activated organelle sorting (FOS). Single organelle sorting has been applied to various organelles to determine the characteristics of individual organelle (Böck et al., 1997). The use of fluorescent organelle cytometry attracted scientists' attention to study single mitochondria (Cavelier et al., 2000). In this study, we took the advantage of single organelle sorting to improve the purity of mitochondria sample. After the FOS, the presence of the mitochondrion and the apicoplast genomic DNAs in the GFP positive fraction recovered was confirmed by PCR with target specific primers. This result indicates that applying different mode of fractionation, mitochondria and apicoplast were, again, co-fractionated. Our results strongly suggest that the mitochondrion and the apicoplast of *P. falciparum* are bound to each other.

Up to date, study of mitochondrion and apicoplast of *Plasmodium* has been restricted to the whole cell, and physical interaction between two organelles had not been determined. The extensive genomic information from malaria genome project (Gardner et al., 2002) provided ideas about the putative metabolic pathway in mitochondria and apicoplast in *P. falciparum*. Among those pathways, heme biosynthesis is unique one as the pathway is predicted to begin in the mitochondrion but subsequent reactions are likely taken place in the apicoplast; 5-aminolevulinic acid (ALA), the first intermediate of the pathway, seemed to be synthesized in the mitochondrion via Shemin pathway but converted to porphobilinogen, the next intermediate, in the apicoplast. This peculiarity was experimentally confirmed by localizing ALA synthase and porphobilinogen synthase (ALA dehydratase), respectively (Sato et al., 2004). The parasite may have a requirement to locate these two organelles in a close proximity to facilitate transport of ALA from the mitochondrion to the apicoplast.

The mitochondrion and the apicoplast of *Plasmodium* spp. have been observed in a proximity to each other by electron microscopy and fluorescent microscopy (Aikawa, 1966; Hopkins et al., 1999; Sato et al., 2004; van Dooren et al., 2005), however the strength in the interaction might vary depending on the parasite stage. It is possible that interaction between apicoplast and mitochondrion to be disrupted in the process of mitochondria preparation.

Despite of extensive observations, it is still unknown if there is a significant structure directly connecting these organelles, like tight junction. These organelles can be connected indirectly, e.g., through the cytoskeleton. Both organelles were recovered not only in the fractions forming the second peak with the DHOD activity but also in those forming the first peak after our Percoll centrifugation (Fig. 2). This may suggest that the putative connection between the organelles has a complex structure involving plenty of auxiliary proteins in a physiological state, but can be reduced to a simple, basic structure that is still capable to hold both organelles together.

Acknowledgements

The authors thank late Dr. Masamichi Aikawa for comments on morphological observations by electron microscopy and wish to dedicate this paper to him. The blood and plasma used in this study is a kind donation from Tokyo Metropolitan Red Cross Blood Centre. WR99210, the drug used for the screening of transfected parasites was a kind gift from Jacobus Pharmaceutical Co., Inc. This study was supported by a Grant-in-Aid for scientific research on priority areas and for Creative Scientific Research from the Japanese Ministry of Education, Science, Culture, and Sports (13226015, 13854011, 17209013, 17590368, 18073004 and 18GS0314) and for research on emerging and re-emerging infectious diseases from the Japanese Ministry of Health and Welfare, and by British Medical Research Council.

References

Aikawa, M., 1966. The fine structure of the erythrocytic stages of three avian malarial parasites, *Plasmodium fallax*, *P. lophurae* and *P. cathemerium*. Am. J. Trop. Med. Hyg. 15, 449–471.

Bannister, L.H., Hopkins, J.M., Fowler, R.E., Krishna, S., Mitchell, G.H., 2000. A brief illustrated guide to the ultrastructure of *Plasmodium falciparum* asexual blood stages. Parasitol. Today 16, 427–433.

Böck, G., Steinlein, P., Huber, L.A., 1997. Cell biologists sort things out: analysis and purification of intracellular organelles by flow cytometry. Trends Cell Biol. 7, 499–503.

Bradford, M.M., 1976. A rapid and sensitive method for the quantitation of microgram quantities of protein utilizing the principle of protein–dye binding. Anal. Biochem. 72, 248–254.

Cavelier, L., Johannisson, A., Gyllensten, U., 2000. Analysis of mtDNA copy number and composition of single mitochondrial particles using flow cytometry and PCR. Exp. Cell Res. 259, 79–85.

Feagin, J.E., 1992. The 6-kb element of *Plasmodium falciparum* encodes mitochondrial cytochrome genes. Mol. Biochem. Parasitol. 52, 145–148.

Fry, M., Beesley, J.E., 1991. Mitochondria of mammalian *Plasmodium* spp.. Parasitology 102, 17–26.

Gardner, M.J., Hall, N., Fung, E., White, O., Berriman, M., Hyman, R.W., Carlton, J.M., Pain, A., Nelson, K.E., Bowman, S., Paulsen, I.T., James, K., Eisen, J.A., Rutherford, K., Salzberg, S.L., Craig, A., Kyes, S., Chan, M.S., Nene, V., Shallom, S.J., Suh, B., Peterson, J., Angiuoli, S., Pertea, M., Allen, J., Selengut, J., Haft, D., Mather, M.W., Vaidya, A.B., Martin, D.M., Fairlamb, A.H., Fraunholz, M.J., Roos, D.S., Ralph, S.A., McFadden, G.I., Cummings, L.M., Subramanian, G.M., Mungall, C., Venter, J.C., Carucci, D.J., Hoffman, S.L., Newbold, C., Davis, R.W., Fraser, C.M., Barrell, B., 2002. Genome sequence of the human malaria parasite *Plasmodium falciparum*. Nature 419, 498–511.

Gardner, M.J., Bishop, R., Shah, T., de Villiers, E.P., Carlton, J.M., Hall, N., Ren, Q., Paulsen, I.T., Pain, A., Berriman, M., Wilson, R.J.M., Sato, S., Ralph, S.A., Mann, D.J., Xiong, Z., Shallom, S.J., Weidman, J., Jiang, L., Lynn, J., Weaver, B., Shoaibi, A., Domingo, A.R., Wasawo, D., Crabtree, J., Wortman, J.R., Haas, B., Angiuoli, S.V., Creasy, T.H., Lu, C., Suh, B., Silva, J.C., Utterback, T.R., Feldblyum, T.V., Pertea, M., Allen, J., Nierman, W.C., Taracha, E.L., Salzberg, S.L., White, O.R., Fitzhugh, H.A., Morzaria, S., Venter, J.C., Fraser, C.M., Nene, V., 2005. Genome sequence of *Theileria parva*, a bovine pathogen that transforms lymphocytes. Science 309, 134–137.

Gero, A.M., Brown, G.V., O'Sullivan, W.J., 1984. Pyrimidine de novo synthesis during the life cycle of the intraerythrocytic stage of *Plasmodium falciparum*. J. Parasitol. 70, 536–541.

Greenwood, B.M., Bojang, K., Whitty, C.J., Targett, G.A., 2005. Malaria. Lancet 365, 487–498.

Gutteridge, W.E., Trigg, P.I., 1970. Incorporation of radioactive precursors into DNA and RNA of *Plasmodium knowlesi in vitro*. J. Protozool. 17, 89–96.

Hopkins, J., Fowler, R., Krishna, S., Wilson, I., Mitchell, G., Bannister, L., 1999. The plastid in *Plasmodium falciparum* asexual blood stages: a three-dimensional ultrastructural analysis. Protist 150, 283–295.

Kohler, S., Delwiche, C.F., Denny, P.W., Tilney, L.G., Webster, P., Wilson, R.J.M., Palmer, J.D., Roos, D.S., 1997. A plastid of probable green algal origin in Apicomplexan parasites. Science 275, 1485–1489.

Krungkrai, J., 1995. Purification, characterization and localization of mitochondrial dihydroorotate dehydrogenase in *Plasmodium falciparum*, human malaria parasite. Biochim. Biophys. Acta 1243, 351–360.

Krungkrai, J., Krungkrai, S.R., Suraveratum, N., Prapunwattana, P., 1997. Mitochondrial ubiquinol-cytochrome *c* reductase and cytochrome *c* oxidase: chemotherapeutic targets in malarial parasites. Biochem. Mol. Biol. Int. 42, 1007–1014.

Lambros, C., Vanderberg, J.P., 1979. Synchronization of *Plasmodium falciparum* erythrocytic stages in culture. J. Parasitol. 65, 418–420.

Mi-Ichi, F., Miyadera, H., Kobayashi, T., Takamiya, S., Waki, S., Iwata, S., Shibata, S., Kita, K., 2005. Parasite mitochondria as a target of chemotherapy: inhibitory effect of licochalcone A on the *Plasmodium falciparum* respiratory chain. Ann. N. Y. Acad. Sci. 1056, 46–54.

Prapunwattana, P., O'sullivan, W.J., Yuthavong, Y., 1988. Depression of *Plasmodium falciparum* dihydroorotate dehydrogenase activity in *in vitro* culture by tetracycline. Mol. Biochem. Parasitol. 27, 119–124.

Ralph, S.A., van Dooren, G.G., Waller, R.F., Crawford, M.J., Fraunholz, M.J., Foth, B.J., Tonkin, C.J., Roos, D.S., McFadden, G.I., 2004. Metabolic maps and functions of the *Plasmodium falciparum* apicoplast. Nat. Rev. 2, 203–216.

Roth Jr., E.F., Calvin, M.C., Max-Audit, I., Rosa, J., Rosa, R., 1988. The enzymes of the glycolytic pathway in erythrocytes infected with *Plasmodium falciparum* malaria parasites. Blood 72, 1922–1925.

Sato, S., Rangachari, K., Wilson, R.J.M., 2003. Targeting GFP to the malarial mitochondrion. Mol. Biochem. Parasitol. 130, 155–158.

Sato, S., Clough, B., Coates, L., Wilson, R.J., 2004. Enzymes for heme biosynthesis are found in both the mitochondrion and plastid of the malaria parasite *Plasmodium falciparum*. Protist 155, 117–125.

Sherman, I.W., 1979. Biochemistry of Plasmodium (malaria parasite). Microbiol. Rev. 43, 453–495.

Srivastava, I.K., Rottenberg, H., Vaidya, A.B., 1997. Atovaquone, a broad spectrum antiparasitic drug, collapses mitochondrial membrane potential in a malarial parasite. J. Biol. Chem. 272, 3961–3966.

Srivastava, I.K., Morrisey, J.M., Darrouzet, E., Daldal, F., Vaidya, A.B., 1999. Resistance mutations reveal the atovaquone-binding domain of cytochrome *b* in malaria parasites. Mol. Microbiol. 33, 704–711.

Slomianny, C., Prensier, G., 1986. Application of the serial sectioning and tridimensional reconstruction techniques to the morphological study of the *Plasmodium falciparum* mitochondrion. J. Parasitol. 72, 595–598.

Suraveratum, N., Krungkrai, S.R., Leangaramgul, P., Prapunwattana, P., Krungkrai, J., 2000. Purification and characterization of *Plasmodium falciparum* succinate dehydrogenase. Mol. Biochem. Parasitol. 105, 215–222.

Takashima, E., Takamiya, S., Takeo, S., Mi-ichi, F., Amino, H., Kita, K., 2001. Isolation of mitochondria from *Plasmodium falciparum* showing dihydroorotate dependent respiration. Parasitol. Int. 50, 273–278.

Takeo, S., Kokaze, A., Ng, C.S., Mizuchi, D., Watanabe, J.I., Tanabe, K., Kojima, S., Kita, K., 2000. Succinate dehydrogenase in *Plasmodium falciparum* mitochondria: molecular characterization of the SDHA and SDHB genes for the catalytic subunits, the flavoprotein (Fp) and iron–sulfur (Ip) subunits. Mol. Biochem. Parasitol. 107, 191–205.

Tan, T.M., Nelson, J.S., Ng, H.C., Ting, R.C., Kara, U.A., 1997. Direct PCR amplification and sequence analysis of extrachromosomal Plasmodium DNA from dried blood spots. Acta Trop. 68, 105–114.

Trager, W., Jensen, J.B., 1976. Human malaria parasites in continuous culture. Science 193, 673–675.

Vaidya, A.B., Akella, R., Suplick, K., 1989. Sequences similar to genes for two mitochondrial proteins and portions of ribosomal RNA in tandemly arrayed 6-kilobase-pair DNA of a malarial parasite. Mol. Biochem. Parasitol. 35, 97–107.

van den Hoff, M.J., Moorman, A.F., Lamers, W.H., 1992. Electroporation in 'intracellular' buffer increases cell survival. Nucleic Acids Res. 20, 2902.

van Dooren, G.G., Marti, M., Tonkin, C.J., Stimmler, L.M., Cowman, A.F., McFadden, G.I., 2005. Development of the endoplasmic reticulum, mitochondrion and apicoplast during the asexual life cycle of *Plasmodium falciparum*. Mol. Microbiol. 57, 405–419.

Vincent, R., Nadeau, D., 1983. A micromethod for the quantitation of cellular proteins in Percoll with the Coomassie brilliant blue dye-binding assay. Anal. Biochem. 135, 355–362.

Vollmer, M., Thomsen, N., Wiek, S., Seeber, F., 2001. Apicomplexan parasites possess distinct nuclear-encoded, but apicoplast-localized, plant-type ferredoxin-NADP$^+$ reductase and ferredoxin. J. Biol. Chem. 276, 5483–5490.

Wilson, R.J., Fry, M., Gardner, M.J., Feagin, J.E., Williamson, D.H., 1992. Subcellular fractionation of the two organelle DNAs of malaria parasites. Curr. Genet. 21, 405–408.

Wilson, R.J.M., Denny, P.W., Preiser, P.R., Rangachari, K., Roberts, K., Roy, A., Whyte, A., Strath, M., Moore, D.J., Moore, P.W., Williamson, D.H., 1996. Complete gene map of the plastid-like DNA of the malaria parasite *Plasmodium falciparum*. J. Mol. Biol. 261, 155–172.

Review TRENDS in Parasitology Vol.23 No.5

Parasitology in Japan

Advances in drug discovery and biochemical studies

Kiyoshi Kita[1], Kazuro Shiomi[2] and Satoshi Ōmura[2]

[1] Department of Biomedical Chemistry, Graduate School of Medicine, The University of Tokyo, Tokyo 113-0033, Japan
[2] Kitasato Institute for Life Sciences, Kitasato University and The Kitasato Institute, Minato-ku, Tokyo 108-8641, Japan

Japanese researchers continue to discover new means to combat parasites and make important contributions toward developing tools for global control of parasitic diseases. *Streptomyces avermectinius*, the source of ivermectin, was discovered in Japan in the early 1970s and renewed and vigorous screening of microbial metabolites in recent years has led to the discovery of new antiprotozoals and anthelminthics, including antimalarial drugs. Intensive studies of parasite energy metabolism, such as NADH–fumarate reductase systems and the synthetic pathways of nucleic acids and amino acids, also contribute to the identification of novel and unique drug targets.

Parasitology in Japan: pioneering aspects

Japanese researchers have had a long and successful history in the field of parasitology, perhaps best exemplified by the accomplishments of Kitasato. In establishing a personal and long-term collaboration with Koch and other European researchers and institutes, Kitasato paved the way for numerous compatriots to follow. He also recognized that the public and private sectors had differing but equally important contributions to make in the battle to understand and conquer parasitic diseases. The first man-made chemotherapeutic compound, trypan red, was discovered by Ehrlich and Shiga, who was sent to work alongside Ehrlich from Kitasato's research group in Japan [1]. Trypan red (Figure 1) was effective against trypanosomal infections of mice and its analog, suramin, is still an important drug in human African trypanosomiasis. In Japan, several key infectious diseases, such as malaria and schistosomiasis, have been eliminated and the first successful eradication of filariasis was accomplished in the 1970s by mass administration of the drug diethylcarbamazine [2,3]. Ivermectin, one of the most effective antiparasite drugs, also originated in Japan. This article focuses on recent progress in Japan on novel antiparasite-drug discovery and recent biochemical studies of parasite metabolism that indicate potential new drug targets (Table 1).

Antiprotozoan and metazoan compounds

In Japan, the search for antiparasitic drugs began in earnest in 1922 when Nishi *et al.* produced antimony sodium tartrate (Stibnal®) and showed its effect on *Schistosoma japonicum* [4]. The sodium salt proved less toxic than the previously reported potassium salt. Santonin was isolated from the flower of *Artemisia cina* and used for ascariasis control [5]. It was isolated by Nippon Shinyaku Company Ltd (http://www.nippon-shinyaku.co.jp/) from *Artemisia maritima* in the late 1920s and has been used commercially in Japan since 1940 [6].

New antimetazoans

After World War II, Japan witnessed a flurry of intensive scientific activity and breakthroughs in the fight against parasitic diseases, which resulted in the development of several important antimetazoan-parasite drugs. For example, Yokogawa *et al.* discovered the effectiveness of bithionol in the chemotherapy of paragonimiasis [7] and it was widely used for trematode and cestode infections before praziquantel. Kainic acid, which was isolated from the red alga *Digenea simplex* by Murakami *et al.* [8], was used against some nematode infections as a mixture with santonin. Destomycin A, which is produced by the actinomycete *Streptomyces rimofaciens* and was isolated by Meiji Seika Kaisha Ltd (http://www.meiji.co.jp) [9], is an aminoglycoside that is used for the treatment of nematode infections in the veterinary field.

Isolated by Meiji Seika in the 1990s, PF1022A is a highly effective compound: a cyclic octadepsipeptide nematocide that is produced by the fungus *Rosellinia* spp. [10]. Emodepside, a semisynthetic derivative of PF1022A with a morpholine ring at each of the two D-phenyllactic acids in the para position [11], was later developed by Bayer HealthCare (http://www.bayerhealthcare.com), Meiji Seika and Astellas Pharma Inc. (http://www.astellas.com). Its target was identified as a novel 110 kDa heptahelical transmembrane receptor, named HC-110R, which is similar to mammalian latrophilins [12]. Latrophilins are latrotoxin (black widow spider venom) receptors and G-protein-coupled receptors that are implicated in the regulation of exocytosis. Latrotoxin also binds to HC110-R and causes influx of external Ca^{2+}. Emodepside works as an antagonist to latrotoxin signaling by impairing the influx of Ca^{2+}. It is highly effective against adult stages of the nematodes *Nippostrongylus brasiliensis* and *Strongyloides ratti* in rats and the nematode *Heligmosomoides polygyrus* in mice when used at an oral-dosage range of 1.0–10 mg/kg [11]. It can counteract resistance against the usual classes of anthelmintics and

Corresponding author: Ōmura, S. (omura-s@kitasato.or.jp).
Available online 23 March 2007.

www.sciencedirect.com 1471-4922/$ – see front matter doi:10.1016/j.pt.2007.03.005

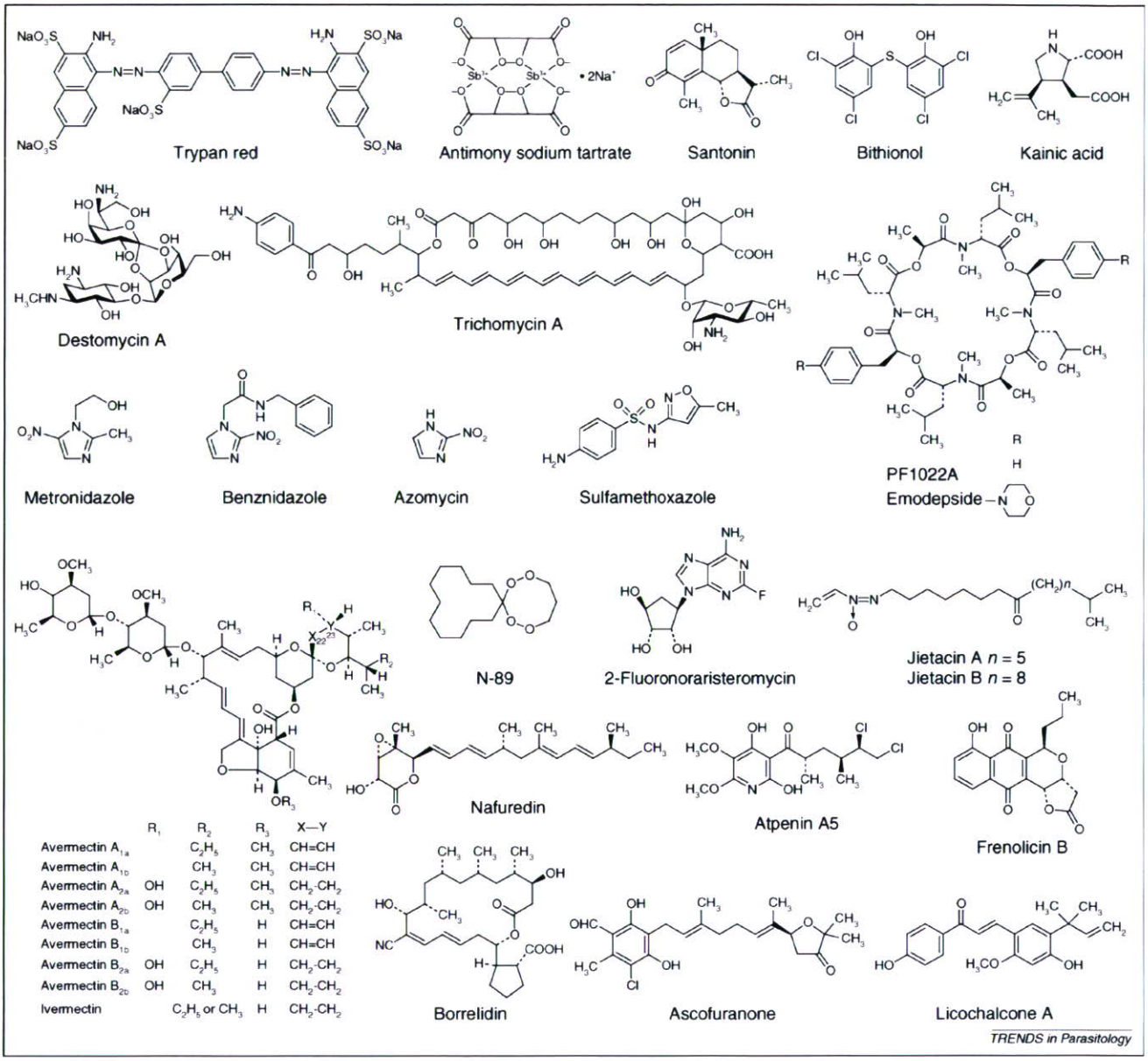

	R_1	R_2	R_3	X—Y
Avermectin A_{1a}		C_2H_5	CH_3	CH=CH
Avermectin A_{1b}		CH_3	CH_3	CH=CH
Avermectin A_{2a}	OH	C_2H_5	CH_3	CH_2-CH_2
Avermectin A_{2b}	OH	CH_3	CH_3	CH_2-CH_2
Avermectin B_{1a}		C_2H_5	H	CH=CH
Avermectin B_{1b}		CH_3	H	CH=CH
Avermectin B_{2a}	OH	C_2H_5	H	CH_2-CH_2
Avermectin B_{2b}	OH	CH_3	H	CH_2-CH_2
Ivermectin		C_2H_5 or CH_3	H	CH_2-CH_2

Figure 1. Structures of antiparasitic compounds that were discovered by Japanese researchers. These compounds are either in current clinical use for parasite diseases or have antiparasitic activity *in vitro* and are good drug candidates. Refs: antimony sodium tartrate [4], ascofuranone [59–62], atpenin A5 [35], avermectins [19–23], azomycin [14,15], benznidazole [71], bithionol [7], borrelidin [38], destomycin A [9], emodepside [11,12], 2-fluoronoraristeromycin [18], frenolicin B [36], ivermectin [24–32], jietacins [33], kainic acid [8], licochalcone A [50], metronidazole [72], N-89 [17], nafuredin [34], PF1022A [10], santonin [5,6], sulfamethoxazole [16], trichomycin A [13], trypan red [1].

was launched in 2005 in Europe as a mixture with praziquantel to eliminate gastrointestinal helminths of cats.

New antiprotozoans

Japan has produced several important antiprotozoan drugs from natural sources. Trichomycin, isolated by Hosoya *et al.*, is used as an antitrichomonal and antifungal antibiotic [13]. It is a mixture of polyene macrolides that are produced by *Streptomyces hachijoensis*. The major component is a 38-membered ring heptaene macrolide, trichomycin A. Nitroimidazole group compounds, such as metronidazole and benznidazole, are derivatives of azomycin, which was isolated from the culture broth of *Streptomyces eurocidicus* by Umezawa *et al.* [14]. After the antitrichomonal activity of azomycin was reported, many such nitroimidazole compounds were then synthesized [15]. Sulfamethoxazole is a sulfa drug that was developed by Shionogi and Company (http://www.shionogi.co.jp) [16] and when mixed with trimethoprim is used as an antibacterial and used for the prevention and treatment of *Pneumocystis carinii*. Recently, several antimalarial candidates have been found by Japanese researchers. Cyclic peroxides with two peroxide groups in the same ring were synthesized by Wataya *et al.* and Nojima *et al.* to be analogous with artemisinin [17]. Among them, N-89 (1,2,6,7-tetraoxaspiro[7.11]nonadecane) showed antimalarial activity comparable to that of artemisinin both *in vitro* and *in vivo* and it cured infection with no parasite

Table 1. Japanese achievements in drug discovery and biochemical studies of parasites

	Year	Research group	Refs
Drug discovery			
Trypan red, the first man-made chemotherapeutic compound	1904	Ehrlich and Shiga	[1]
Antimony sodium tartrate for schistosomiasis	1922	Nishi and colleagues	[4]
Isolation of trichomycin from *Streptomyces hachijoensis*	1952	Hosoya and colleagues	[13]
Isolation of azomycin, the origin of nitroimidazoles	1953	Umezawa and colleagues	[14]
Isolation of kainic acid from *Digenea simplex*	1953	Murakami and colleagues	[8]
Synthesis of sulfamethoxazole	1957	Kano and Ogata	[16]
Bithionol for paragonimiasis	1962	Yokogawa and colleagues	[7]
Isolation of destomycin A from *Streptomyces rimofaciens*	1965	Kondō and colleagues	[9]
Isolation of avermectins from *Streptomyces avermectinius*	1979	Ōmura, Burg, Campbell and colleagues	[20,21]
Isolation of PF1022A, the origin of emodepside	1992	Sasaki and colleagues	[10]
Biochemical studies			
Anerobic respiratory chain of *Ascaris suum*	1984	Oya and colleagues	[39]
Trypanosome alternative oxidase and its specific inhibitor, ascofuranone	1996	Kita and colleagues	[59]
Pyrimidine biosynthetic gene cluster	1999	Aoki and colleagues	[51]
Unsaturated fatty acids essential for *Plasmodium* growth	2000	Mitamura and colleagues	[42]
Stage-specific isoforms of *A. suum* complex II	2003	Kita and colleagues	[41]
Peroxiredoxins in *Plasmodium*	2003	Kawazu and colleagues	[46]
Unique metabolism of sulfur-containing amino acids in *Entamoeba histolytica*	2003	Nozaki and colleagues	[63]

recrudescence or toxicity following oral administration in mice. Work has also indicated that *S*-adenosyl-L-homocysteine hydrolase might be a good target for antimalarial drugs. 2-fluoronoraristeromycin, designed by Kitade *et al.*, showed good selectivity for this enzyme in *Plasmodium falciparum* compared with that in humans [18].

Discovery of avermectins and other antiparasitics

Established by its namesake, The Kitasato Institute (KI: http://www.kitasato.or.jp) has a proud history of antibiotics discovery, including leucomycin (kitasamycin) and mitomycin C. Ivermectin is an endectocide that is active against a diverse range of nematodes, insects and arachnids and has its origins in the institute [19]. Ivermectin is now recognized by many as one of the most important drugs in human and animal health of the past century. In 1973, researchers at the KI started to screen nematocidal antibiotics in collaboration with Merck, Sharpe and Dohme Research Laboratories (MSD: http://www.msd.com). The Kitasato group isolated cultures from soil samples and undertook *in vitro* evaluation of the fermentation broths. In the MSD laboratories, promising cultures were screened using a novel model of helminth infection – mice infected with the nematode *Nematospiroides dubius*. The broth of strain MA-4680 exhibited potent anthelmintic activity [20]. This strain originated in a soil sample collected at Kawana, Shizuoka prefecture [21] and was classified as a new species of actinomycetes and named *Streptomyces avermectinius* (formerly *Streptomyces avermitilis*) [22]. Eight active components were isolated from the broth and named avermectins A_{1a}–B_{2b}. Compounds of the B series, which have a 5-hydroxy group, are markedly more active than those of the A series, which have a 5-methoxy group. Reduction of the 22,23-olefin of the most active avermectins B_{1a} and B_{1b} improved both the activity spectrum and the safety and the resulting 22,23-dihydro B_1 complex (as a mixture of 80% B_{1a} and 20% B_{1b}) was marketed as a veterinary drug under the generic and nonproprietary name ivermectin in 1981 [23].

Ivermectin is used for the control of economically important nematodes that infect the gastrointestinal tract, lungs and kidneys, in addition to other nematodes of livestock such as *Thelazia* and *Parafilaria*. It is also used against several arthropod parasites, including grubs, lice, mites and screw worms [24]. In companion animals, it provides good control of *Dirofilaria immitis*. Ivermectin was later found to be safe and highly effective in controlling some nematode infections in humans. Of greatest importance is that it proved highly efficacious against microfilariae of *Onchocerca volvulus*, which causes river blindness. Unique, pioneering and multifaceted public–private partnerships (PPPs) were established and eventually incorporated several United Nations agencies (http://www.un.org) and nongovernmental organizations. These PPPs enabled the donation of ivermectin (under the brand name Mectizan®) and led to a model for a highly successful mass drug administration (MDA) program that should culminate in the elimination of onchocerciasis in the endemic areas of Africa and the Americas [25]. Ivermectin is a remarkably safe and effective broad-spectrum drug. Side effects, when they do occur, are minimal and tolerable, usually resulting from inflammatory and immune defenses that are triggered by immobilized or dead microfilariae [26]. Therefore, ivermectin can be administered by nonmedical individuals after a modicum of training and can be used in MDA programs that are run by affected communities themselves. Although ivermectin is also effective against *Loa loa* [26], a few severe adverse events have occurred in individuals with high levels of *L. loa* microfilariae that have been treated with ivermectin [27]. Recently, ivermectin has also become an invaluable tool for a global elimination initiative against lymphatic filariasis, a disease that is caused by infection with *Wuchereria bancrofti* and *Brugia malayi* [26]. This means that the drug will be available free of charge in order to rid the world of two devastating diseases and to improve the lives of hundreds of millions of people. Ivermectin has now been found to be the most useful agent for strongyloidiasis [28]. In addition to the control of nematode infections, ivermectin also shows efficacy against human scabies, which is caused by infection with the ectoparasitic mite *Sarcoptes scabiei* [29].

Avermectin targets a parasite-specific glutamate-gated chloride channel [30], which it activates to cause neurological disruption of the parasite. Although avermectins also bind to γ-aminobutyric acid-gated and glycine-gated chloride channels in mammals, their affinity for invertebrate receptors is ~100-times higher. Mice that have the P-glycoprotein gene knocked out showed increased sensitivity to ivermectin [31]. This result established an important role for P-glycoprotein in the maintenance of the blood–brain barrier and indicated that the safety of ivermectin is because of the blood–brain barrier, in addition to the low affinity of the receptors.

In 2003, the Kitasato group elucidated the complete genetic sequence of *S. avermectinius* [32]. The genome is the largest bacterial genome yet sequenced (9026 kb) and encodes ≥7574 potential open reading frames. Analysis identified the gene cluster that is involved in secondary-metabolite production and sheds light on the biology of microbial secondary-metabolite synthesis at the genetic level, thus offering the prospect of creating some new metabolites.

After the discovery of avermectin, the Kitasato group isolated jietacins A and B from the culture broth of *Streptomyces* spp. using the pine wood nematode, *Bursaphelenchus lignicolus* [33]. Jietacins show a ~10-times higher nematocidal activity than avermectin B_{1a} against *B. lignicolus in vitro*. Nafuredin, produced by the fungus *Aspergillus niger*, was found during screening for an NADH–fumarate reductase inhibitor [34]. It inhibits helminth electron transport enzyme complex I and shows anthelmintic activity against *Haemonchus contortus* in sheep (see later). Atpenin A5 was discovered during the same screening and is the most potent complex II inhibitor. It might, therefore, be a useful tool for clarifying the biochemical and structural properties of complex II [35]. In the case of antiprotozoan compounds, frenolicin B, which is produced by *Streptomyces roseofulvus*, has potent anticoccidial activity in *Eimeria tenella* infection in chicks [36].

Building on the increased global awareness that the public and private sectors need to work together if the major communicable diseases are to be overcome, a PPP that includes leading Japanese pharmaceutical companies, the Japanese Ministry of Health, Labour and Welfare, and the World Health Organization was established in 1999 to discover new antimalarials [37] and is collectively known as the JPMW project. A screening center was established at the KI in which evaluation of antimalarial activity of compounds is carried out both *in vitro* and using the rodent malaria model. These compounds come from two sources: those donated from the chemical libraries of 14 Japanese companies and natural products from the KI. More than 30 000 compounds have been screened since 2000 and one compound, borrelidin, shows excellent antimalarial activity in both *in vitro* chloroquine (CQ)-susceptible and CQ-resistant *P. falciparum* models [38]. It also has antimalarial activity against rodent malaria. The effective dose is lower than that required for artemether, artesunate and CQ itself. The 90% effective dose (ED_{90}) values of orally-administered borrelidin, artemether, artesunate and CQ against CQ-resistant *P. yoelii*-infected mice were 1.1, 40, >50 and >100 mg/kg, respectively [38].

Elucidation of biochemical targets in protozoan and metazoan parasites

Parasites have developed a range of physiological functions that are necessary for their survival within the specialized environment of the host and studies of these parasitic adaptations have provided interesting biological discoveries [39]. Recent advances in biochemical and molecular biological approaches have provided new knowledge and led to many breakthroughs in the field of biological evolution and parasite diversity, with the novel understanding of unique aspects of parasite metabolism heralding promising targets for chemotherapy.

The anerobic respiratory chain of mitochondria in helminths

Recent research by Kita *et al.* on the respiratory chain of the parasitic helminth *A. suum* has shown that the mitochondrial NADH–fumarate reductase system (Figure 2) has an important role in the anerobic energy metabolism of adult parasites, in addition to unique features of the developmental changes that occur during their life cycle [39]. In this system, the reducing equivalent of NADH is transferred to the low-potential rhodoquinone (RQ) by the NADH–RQ reductase complex (complex I). This pathway ends with the production of succinate by the rhodoquinol–fumarate reductase activity of complex II [succinate–ubiquinone (UQ) reductase in aerobic respiration]. Electron transfer from NADH to fumarate is coupled to site I phosphorylation of complex I by generation of a protonmotive force. The difference in redox potential between the NAD^+–NADH couple ($Em' = -320$ mV) and the fumarate–succinate couple ($Em' = +30$ mV) is sufficiently high to drive ATP synthesis. The anerobic NADH–fumarate reductase system is found not only in nematodes but also in bacteria and many other parasites.

An anthelmintic compound, nafuredin, selectively inhibits helminth complex I at nanomolar concentrations [34]. Kinetic analysis showed that the inhibition by nafuredin is competitive against an exogenous RQ. These findings, coupled with the fact that helminth complex I uses both RQ and UQ as an electron acceptor, indicate that the structural features of the quinone reduction site of helminth complex I might differ from that of mammalian complex I. In fact, the inhibitory mechanism of quinazolines was competitive against RQ and partially competitive against UQ [40].

Amino *et al.* have demonstrated that *A. suum* mitochondria express stage-specific isoforms of complex II: the flavoprotein subunit and the small subunit of cytochrome *b* of the larval complex II differ from those of the adult enzyme, although two complex IIs share a common iron–sulfur cluster subunit [41]. Enzymatic assays indicated that *A. suum* complex IIs have different properties compared with complex IIs of mammalian hosts and that the larval complex II is able to function as a rhodoquinol–fumarate reductase. As mentioned earlier, the most potent inhibitor of complex II, atpenin A5, was found during screening of inhibitors for the *A. suum* complex II [35]. Osanai *et al.* obtained a crystal of adult complex II and an analysis of parasite-specific factors in the enzyme complex is now in progress.

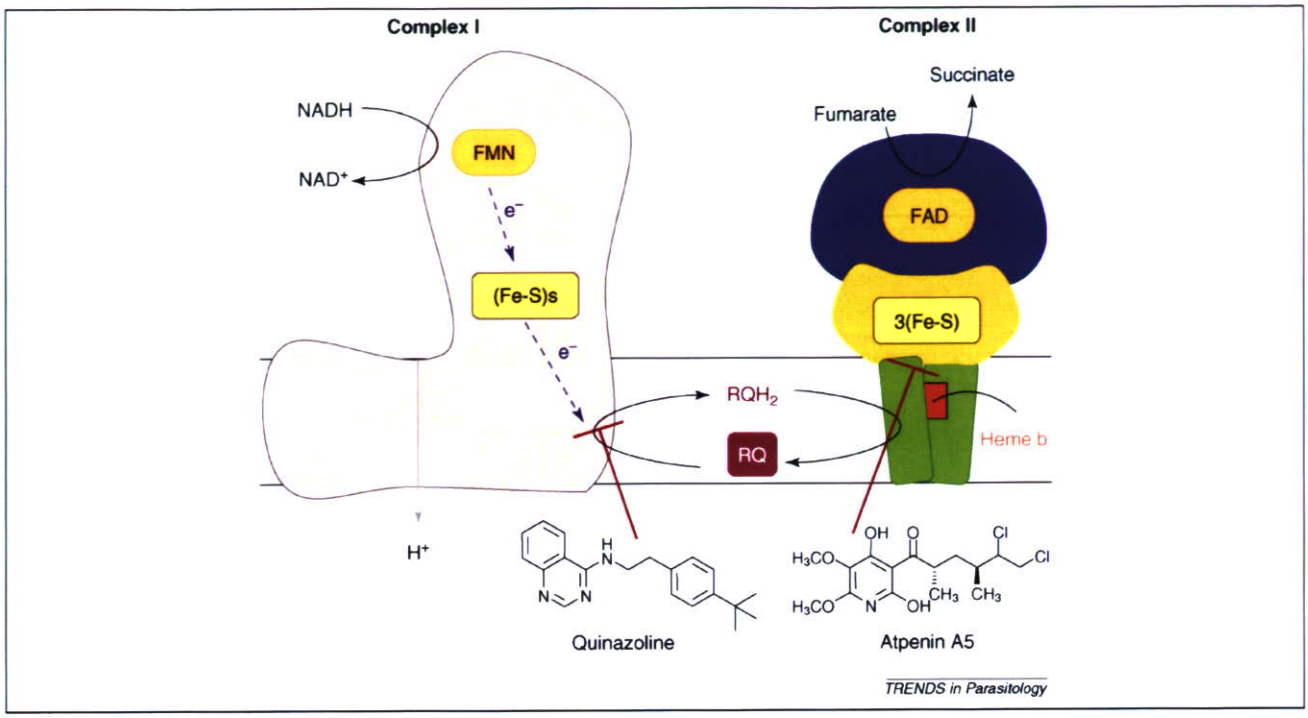

Figure 2. NADH–fumarate reductase system in *Ascaris suum* mitochondria. The respiratory inhibitors quinazoline [40] and atpenin A5 [35] inhibit *A. suum* complex I and complex II, respectively. Nafuredin (see Figure 1) also inhibits *A. suum* complex I [34]. Figure by K. Sakamoto, University of Tokyo.

Unique *Plasmodium* enzymes

P. falciparum is the causative agent for the most severe form of malaria in humans. Because clinical symptoms and complex pathogenesis are exclusively associated with the asexual multiplication of this parasite in erythrocytes, Mitamura and colleagues have focused on intra-erythrocytic proliferation of *P. falciparum* and lipid metabolism and trafficking in parasitized erythrocytes [42]. They found that limited combinations of saturated and unsaturated free fatty acids (the best combination of which is palmitic and oleic acids) are essential serum factors that are required for parasite growth to ensure complete intra-erythrocytic development and cell cycle progression [42]. This finding showed that scavenging free fatty acids from host serum is crucial for the survival of intra-erythrocytic *Plasmodium* parasites. Furthermore, Mitamura and colleagues have shown genetic evidence that *P. falciparum* diacylglycerol acyltransferase 1, a principal enzyme for triacylglycerol biosynthesis, seems to have a crucial role in the intra-erythrocytic proliferation of the parasite [43]. Their work on lipid metabolism and trafficking in *P. falciparum* has attracted attention with respect to both basic biology and its potential application for malaria chemotherapy [44].

Because the parasites do not possess catalase or glutathione peroxidase, the bulk of peroxide-reducing capacity in the cell seems to be provided by peroxiredoxins (Prx) [45]. Kawazu and his group reported that disruption of the gene that encodes the cytosolic 2-Cys Prx (PfTPx-1) in *P. falciparum* renders parasites hypersensitive to reactive oxygen and nitrogen species [46]. They also showed that the other cytosolic Prx (Pf1-Cys-Prx) might help to protect the parasite against oxidative stress that results from hemoglobin metabolism [47]. These findings indicate that parasites use the Prx proteins on different occasions for management of intracellular oxidative stresses during their intra-erythrocytic development [48]. How the parasite regulates proper expression of the antioxidant proteins under different physiological situations is a matter of great interest.

Differences between the mitochondria of malaria parasites and those of the host are also expected to indicate potential targets for chemotherapy. Using active mitochondria that have been isolated from *P. falciparum* [49], Miichi *et al.* investigated the licochalcone A-inhibited bc_1 complex (ubiquinol–cytochrome *c* reductase), in addition to complex II (succinate–ubiquinone reductase) of *P. falciparum* mitochondria [50]. Because the properties of the *P. falciparum* bc_1 complex are different from those of the mammalian host and are a target of atovaquone, chalcones are promising candidates for new antimalarial drugs.

Targets in trypanosomes and ameba

Nara and coworkers reported a novel, polycistronic pyrimidine-biosynthetic (*pyr*) cluster that contains five genes (*pyr1*, *pyr3*, *pyr6–5*, *pyr2* and *pyr4*) and encode all six enzymes that are involved in pyrimidine biosynthesis in *Trypanosoma cruzi* and *Leishmania* spp. [51]. Although most eukaryotes carry *pyr5–6*, kinetoplastids possess the conversely fused *pyr6–5*. This biosynthesis pathway is essential for protozoan survival [52,53]. In particular, the *pyr4*- and *pyr6*-encoded enzymes are promising drug targets because they differ biochemically from those of their mammalian-host counterparts, probably because these genes have been horizontally acquired [53–55]. Phylogenetic studies of the kinetoplastid *pyr6–5* indicated that

multiple gene fusion and fission events have occurred in various eukaryotic groups and this information sheds new light on the evolutionary concept of gene fusion. Crystals of dihydroorotate dehydrogenase, a *pyr4* gene product, were obtained by Inaoka *et al.* and provide important information for structure-based drug design [56]. Hashimoto *et al.* [57,58] reported that *T. cruzi* post-transcriptionally upregulates and exploits host c-FLIP for inhibition of a death-inducing signal. This mechanism enables the parasite to survive and results in Chagas disease. Kita and his group discovered ascofuranone, a novel inhibitor of parasite mitochondrial function. This compound blocks the cyanide-insensitive terminal oxidase of *Trypanosoma brucei brucei* mitochondria, an enzyme also known as trypanosome alternative oxidase [59]. In addition, this compound inhibits trypanosomal growth in heavily-infected mice and is a good lead for the development of new treatments for African trypanosomiasis [60]. The direct evidence that the motif $E(X)_6Y$ is essential for the activity of alternative oxidases (AOXs) was reported by Nakamura *et al.* [61]. AOXs have been found in *Cryptosporidium parvum* in addition to trypanosomes [62].

Nozaki and his group have been working to discover and exploit rational targets for the development of chemotherapeutics against *Entamoeba histolytica* infection. *E. histolytica* possesses unique metabolisms of sulfur-containing amino acids [63], particularly in sulfur-assimilatory *de novo* cysteine biosynthesis and degradation of methionine, homocysteine and cysteine. Methionine γ-lyase, which is the sole enzyme responsible for the degradation of cysteine, is a target for further drug development. Nozaki also showed unique aspects in vesicular trafficking that are involved in phagocytosis and intracellular transport of virulence factors, including cysteine proteases in *E. histolytica* [64–69]. The diversity of Rab small GTPases and isoprenylation enzymes of Ras, Rho/Rac and Rab small GTPases involved in the related processes seem to represent divergent and rational targets [70]. In particular, both farnesyltransferase and geranylgeranyltransferase I of *E. histolytica* were proven to be biochemically divergent in their sensitivity to known inhibitors.

Concluding remarks

Essential parasite-specific systems that differ from those of the host represent attractive targets for specialized chemotherapy, as illustrated by glutamate-gated chloride channels and the specific activator avermectin. Many people in developing countries still suffer or die from malaria, schistosomiasis, filariasis and other infectious diseases, whereas, in developed countries, parasitic infectious diseases, especially those that are caused by opportunistic infection resulting from immunosuppressants and HIV/AIDS, are increasing. Moreover, the emergence of strains that are resistant to the current front-line drugs is exacerbating an increasingly dire situation. Therefore, through the knowledge and understanding gained from basic research into parasites and the development of this research for clinical application, Japanese scientists have an important role at the forefront of the control of emerging and re-emerging parasitic diseases.

References

1 Ehrlich, P. and Shiga, K. (1904) Farbentherapeutische versuche bei Trypanosomenerkrankung. *Berlin Klin. Wochenschrift* 41, pp. 329–332 and pp. 362–365
2 Kagei, N. and Hayashi, S. (1999) Control of parasitoses in Japan. In *Progress of Medical Parasitology in Japan* (Vol. 7, Japanese edn) (Otsuru, M. *et al.*, eds), pp. 647–668, Meguro Parasitological Museum
3 Ichimori, K. *et al.* Lymphatic filariasis elimination in the Pacific: PacELF replicating Japanese success, *Trends Parasitol.* 23, 36–40
4 Nishi, M. (1922) Experimental treatment for Schistosomiasis japonica by tartar emetic. *J. Jpn. Soc. Int. Med.* 10, 143–145
5 Felter, H.W. and Lloyd, J.U., eds (1898) *King's American Dispensatory* (18th edn), Ohio Valley Co.
6 Suzuka, O. (1987) The domestic production of santonin at Kyoto – a review on H. Ichinose's works. *J. Jpn. His. Pharm.* 22, 7–10
7 Yokogawa, M. *et al.* (1963) Chemotherapy of paragonimiasis with bithionol v. studies on the minimum effective dose and changes in abnormal X-ray shadows in the chest after treatment. *Am. J. Trop. Med. Hyg.* 12, 859–869
8 Murakami, S. *et al.* (1953) Effective principle of *Digenea*. *Jpn. J. Pharm. Chem.* 25, 571–574
9 Kondō, S. *et al.* (1965) Destomycins A and B, two new antibiotics produced by *Streptomyces*. *J. Antibiot. Ser. A* 18, 38–42
10 Sasaki, T. *et al.* (1992) A new anthelmintic cyclodepsipeptide, PF1022A. *J. Antibiot. (Tokyo)* 45, 692–697
11 Harder, A. and von Samson-Himmelstjerna, G. (2002) Cyclooctadepsipeptides – a new class of anthelmintically active compounds. *Parasitol. Res.* 88, 481–488
12 Saeger, B. *et al.* (2001) Latrophilin-like receptor from the parasitic nematode *Haemonchus contortus* as target for the anthelmintic depsipeptide PF1022A. *FASEB J.* 15, 1332–1334
13 Hosoya, S. *et al.* (1952) Trichomycin, a new antibiotic produced by *Streptomyces hachijoensis* with trichomonadicidal and antifungal activity. *Jpn. J. Exp. Med.* 22, 505–509
14 Maeda, K. *et al.* (1953) A new antibiotic, azomycin. *J. Antibiot. Ser. A* 6, 182
15 Horie, H. (1956) Anti-trichomonas effect of azomycin. *J. Antibiot. (Tokyo)* 9, 168
16 Kano, H. and Ogata, K. (1957) Isoxazole derivatives. X. Synthesis of 5-methyl-3-sulfanilamidoisoxazole. *Ann. Rept. Shionogi Res. Lab.* 7, 1–5
17 Kim, H-S. *et al.* (2001) Synthesis and antimalarial activity of novel medium-sized 1,2,4,5-tetraoxacycloalkanes. *J. Med. Chem.* 44, 2357–2361
18 Kitade, Y. *et al.* (2003) Synthesis of 2-fluoronoraristeromycin and its inhibitory activity against *Plasmodium falciparum* *S*-adenosyl-L-homocysteine hydrolase. *Bioorg. Med. Chem. Lett.* 13, 3963–3965
19 Ōmura, S. and Crump, A. (2004) The life and times of ivermectin – a success story. *Nat. Rev. Microbiol.* 2, 984–989
20 Egerton, J.R. *et al.* (1979) Avermectins, new family of potent anthelmintic agents: efficacy of the B_{1a} component. *Antimicrob. Agents Chemother.* 15, 372–378
21 Burg, R.W. *et al.* (1979) Avermectins, new family of potent anthelmintic agents: producing organism and fermentation. *Antimicrob. Agents Chemother.* 15, 361–367
22 Takahashi, Y. *et al.* (2002) *Streptomyces avermectinius* sp. nov., an avermectin-producing strain. *Int. J. Syst. Evol. Microbiol.* 52, 2163–2168
23 Chabala, J.C. *et al.* (1980) Ivermectin, a new broad-spectrum antiparasitic agent. *J. Med. Chem.* 23, 1134–1136
24 Shoop, W. and Soll, M. (2002) Ivermectin, abamectin and eprinomectin. In *Macrocyclic Lactones in Antiparasitic Therapy* (Vercruysse, J. and Rew, R.S., eds), pp. 1–29, CABI Publishing
25 Richards, F.O. *et al.* (2001) Control of onchocerciasis today: status and challenges. *Trends Parasitol.* 17, 558–563
26 Richard-Lenoble, D. *et al.* (2003) Ivermectin and filariasis. *Fundam. Clin. Pharmacol.* 17, 199–203
27 Geary, T.G. (2005) Ivermectin 20 years on: maturation of a wonder drug. *Trends Parasitol.* 21, 530–532
28 Zaha, O. *et al.* (2002) Ivermectin in clinical practice. In *Macrolide Antibiotics. Chemistry, Biology, and Practice* (2nd edn) (Ōmura, S., ed.), pp. 403–419, Academic Press
29 Heukelbach, J. and Feldmeier, H. (2006) Scabies. *Lancet* 367, 1767–1774

30 Ōmura, S. (2002) Mode of action of avermectin. In *Macrolide Antibiotics. Chemistry, Biology, and Practice* (2nd edn) (Ōmura, S., ed.), pp. 571–576, Academic Press
31 Schinkel, A.H. *et al.* (1994) Disruption of the mouse *mdr1a* P-glycoprotein gene leads to a deficiency in the blood–brain barrier and to increased sensitivity to drugs. *Cell* 77, 491–502
32 Ikeda, H. *et al.* (2003) Complete genome sequence and comparative analysis of the industrial microorganism *Streptomyces avermitilis*. *Nat. Biotechnol.* 21, 526–531
33 Ōmura, S. *et al.* (1987) Jietacins A and B, new nematocidal antibiotics from a *Streptomyces* sp. Taxonomy, isolation, and physico-chemical and biological properties. *J. Antibiot. (Tokyo)* 40, 623–629
34 Ōmura, S. *et al.* (2001) An anthelmintic compound, nafuredin, shows selective inhibition of complex I in helminth mitochondria. *Proc. Natl. Acad. Sci. U. S. A.* 98, 60–62
35 Miyadera, H. *et al.* (2003) Atpenins, potent and specific inhibitors of mitochondrial complex II (succinate–ubiquinone oxidoreductase). *Proc. Natl. Acad. Sci. U. S. A.* 100, 473–477
36 Ōmura, S. *et al.* (1985) Anticoccidial activity of frenolicin B and its derivatives. *J. Antibiot. (Tokyo)* 38, 1447–1448
37 Crump, A. and Otoguro, K. (2005) Satoshi Ōmura: in pursuit of nature's bounty. *Trends Parasitol.* 21, 126–132
38 Otoguro, K. *et al.* (2003) *In vitro* and *in vivo* antimalarial activities of a non-glycosidic 18-membered macrolide antibiotic, borrelidin, against drug-resistant strains of Plasmodia. *J. Antibiot. (Tokyo)* 56, 727–729
39 Kita, K. and Takamiya, S. (2002) Electron transfer complexes in *Ascaris* mitochondria. *Adv. Parasitol.* 51, 95–131
40 Yamashita, T. *et al.* (2004) Rhodoquinone reaction site of mitochondrial complex I, in parasitic helminth, *Ascaris suum*. *Biochim. Biophys. Acta, (Bioenergetics)* 1608, 97–103
41 Amino, H. *et al.* (2003) Isolation and characterization of the stage-specific Cytochrome b small subunit (CybS) of *Ascaris suum* complex II from the aerobic respiratory chain of larval mitochondria. *Mol. Biochem. Parasitol.* 128, 175–186
42 Mitamura, T. *et al.* (2000) Serum factor governing intraerythrocytic development and cell cycle progression of *Plasmodium falciparum*. *Parasitol. Int.* 49, 219–229
43 Placpac, N.M. *et al.* (2004) Evidence that *Plasmodium falciparum* diacylglycerol acyltransferase is essential for intraerythrocytic proliferation. *Biochem. Biophys. Res. Commun.* 321, 1062–1068
44 Mitamura, T. and Placpac, N. (2003) Lipid metabolism in *Plasmodium falciparum*-infected erythrocyte: possible new targets for malaria chemotherapy. *Microbes Infect.* 5, 545–552
45 Müller, S. (2004) Redox and antioxidant systems of the malaria parasite *Plasmodium falciparum*. *Mol. Microbiol.* 53, 1291–1305
46 Komaki-Yasuda, K. *et al.* (2003) Disruption of the *Plasmodium falciparum* 2-Cys peroxiredoxin gene renders parasites hypersensitive to reactive oxygen and nitrogen species. *FEBS Lett.* 547, 140–144
47 Kawazu, S. *et al.* (2005) Roles of 1-Cys peroxiredoxin in heme detoxification in the human malaria parasite *Plasmodium falciparum*. *FEBS J.* 272, 1784–1791
48 Yano, K. *et al.* (2005) Expression of mRNAs and proteins for peroxiredoxins in *Plasmodium falciparum* erythrocytic stage. *Parasitol. Int.* 54, 35–41
49 Takashima, E. *et al.* (2001) Isolation of mitochondria from *Plasmodium falciparum* showing dihydroorotate dependent respiration. *Parasitol. Int.* 50, 273–278
50 Mi-ichi, F. *et al.* (2005) Parasite mitochondria as a target of chemotherapy: The inhibitory effect of licochalcone A on the Plasmodium falciparum respiratory chain. *Ann. N. Y. Acad. Sci.* 1056, 46–54
51 Gao, G. *et al.* (1999) Novel organization and sequences of five genes encoding all six enzymes for *de novo* pyrimidine biosynthesis in *Trypanosoma cruzi*. *J. Mol. Biol.* 285, 149–161
52 Aoki, T. (2003) Metabolism of parasitic protozoa. In *Progress of Medical Parasitology in Japan* (Vol. 7) (Otsuru, M. *et al.*, eds), pp. 175–191, Meguro Parasitological Museum
53 Annoura, T. *et al.* (2005) The origin of dihydroorotate dehydrogenase genes of kinetoplastids, with special reference to their biological significance and adaptation to anaerobic, parasitic conditions. *J. Mol. Evol.* 60, 113–127
54 Nara, T. *et al.* (2005) Inhibitory action of marine algae extracts on the *Trypanosoma cruzi* dihydroorotate dehydrogenase activity and on the protozoan growth in mammalian cells. *Parasitol. Int.* 54, 59–64
55 Sariego, I. *et al.* (2006) Genetic diversity and kinetic properties of *Trypanosoma cruzi* dihydroorotate dehydrogenase isoforms. *Parasitol. Int.* 55, 11–16
56 Inaoka, K. *et al.* (2005) Expression, purification, and crystallization of *Trypanosoma cruzi* dihydroorotate dehydrogenase complexed with orotate. *Acta Crystallogr. F61* 875–878
57 Nakajima-Shimada, J. *et al.* (2000) Inhibition of Fas-mediated apoptosis by *Trypanosoma cruzi* infection. *Biochim. Biophys. Acta* 1475, 175–183
58 Hashimoto, M. *et al.* (2005) *Trypanosoma cruzi* post-transcriptionally upregulates and exploits cellular FLIP for inhibition of death-inducing signal. *Mol. Biol. Cell* 16, 3521–3528
59 Nihei, C. *et al.* (2002) Trypanosome alternative oxidase as a target of chemotherapy. *Biochim. Biophys. Acta* 1587, 234–239
60 Yabu, Y. *et al.* (2006) Chemotherapeutic efficacy of ascofuranone in *Trypanosoma vivax*-infected mice without glycerol. *Parasitol. Int.* 55, 39–43
61 Nakamura, K. *et al.* (2005) Mutational analysis of the *Trypanosoma vivax* alternative oxidase: the $E(X)_6Y$ motif is conserved in both mitochondrial alternative oxidase and plastid terminal oxidase and is indispensable for enzyme activity. *Biochem. Biophys. Res. Commun.* 334, 593–600
62 Suzuki, T. *et al.* (2004) Direct evidence for cyanide insensitive quinol oxidase (alternative oxidase) in apicomplexan parasite *Cryptosporidium parvum*: phylogenetic and therapeutic implication. *Biochem. Biophys. Res. Commun.* 313, 1044–1052
63 Nozaki, T. *et al.* (2005) Sulfur-containing amino acid metabolism in parasitic protozoa. *Adv. Parasitol.* 60, 1–100
64 Saito-Nakano, Y. *et al.* (2004) Rab5-associated vacuoles play a unique role in phagocytosis of the enteric protozoan parasite *Entamoeba histolytica*. *J. Biol. Chem.* 279, 49497–49507
65 Loftus, B. *et al.* (2005) The genome of the protist parasite *Entamoeba histolytica*. *Nature* 433, 865–868
66 Okada, M. *et al.* (2005) Proteomic analysis of phagocytosis in the enteric protozoan parasite *Entamoeba histolytica*. *Eukaryot. Cell* 4, 827–831
67 Nakada-Tsukui, K. *et al.* (2005) A retromerlike complex is a novel Rab7 effector that is involved in the transport of the virulence factor cysteine protease in the enteric protozoan parasite *Entamoeba histolytica*. *Mol. Biol. Cell* 16, 5294–5303
68 Okada, M. and Nozaki, T. (2006) New insights into molecular mechanisms of phagocytosis in *Entamoeba histolytica* by proteomic analysis. *Arch. Med. Res.* 37, 244–251
69 Nozaki, T. and Nakada-Tsukui, K. (2006) Membrane trafficking as a virulence mechanism of the enteric protozoan parasite *Entamoeba histolytica*. *Parasitol. Res.* 98, 179–183
70 Makioka, A. *et al.* (2006) Characterization of protein geranylgeranyltransferase I from the enteric protist *Entamoeba histolytica*. *Mol. Biochem. Parasitol.* 145, 216–225
71 Yoneda, S. *et al.* (1977) Some observations on the effect of Ro 7-1051 on *Trypanosoma cruzi*, particularly in cell culture. *Experientia* 33, 1201–1202
72 Cosar, C. and Julou, L. (1959) Activity of 1-(2-hydroxyethyl)-2-methyl-5-nitroimidazole (RP 8823) in experimental *Trichomonas vaginalis* infections. *Ann. Inst. Pasteur* 96, 238–241

ANTIMICROBIAL AGENTS AND CHEMOTHERAPY, Mar. 2007, p. 1071–1077 Vol. 51, No. 3
0066-4804/07/$08.00+0 doi:10.1128/AAC.01186-06

Independent Evolution of Pyrimethamine Resistance in *Plasmodium falciparum* Isolates in Melanesia[▽]

Toshihiro Mita,[1]* Kazuyuki Tanabe,[2] Nobuyuki Takahashi,[1] Takahiro Tsukahara,[1] Hideaki Eto,[1] Lek Dysoley,[1,3] Hiroshi Ohmae,[4] Kiyoshi Kita,[5] Srivicha Krudsood,[6] Sornchai Looareesuwan,[6] Akira Kaneko,[7] Anders Björkman,[7] and Takatoshi Kobayakawa[1]

Department of International Affairs and Tropical Medicine, Tokyo Women's Medical University, Tokyo, Japan[1]; Laboratory of Malariology, Research Institute for Microbial Diseases, Osaka University, Osaka, Japan[2]; The National Center for Parasitology, Entomology and Malaria Control, Phnom Penh, Cambodia[3]; Department of Parasitology, National Institute of Infectious Diseases, Tokyo, Japan[4]; Department of Biomedical Chemistry, Graduate School of Medicine, University of Tokyo, Tokyo, Japan[5]; The Asian Centre of International Parasite Control, Faculty of Tropical Medicine, Mahidol University, Thailand[6]; and Department of Medicine, Malaria Research Laboratory, Karolinska Institutet, Stockholm, Sweden[7]

Received 22 September 2006/Returned for modification 1 December 2006/Accepted 18 December 2006

Pyrimethamine resistance in *Plasmodium falciparum* has previously been shown to have emerged once in Southeast Asia, from where it spread to Africa. Pyrimethamine resistance in this parasite is known to be conferred by mutations in the gene encoding dihydrofolate reductase (*dhfr*). We have analyzed polymorphisms in *dhfr* as well as microsatellite haplotypes flanking this gene in a total of 285 isolates from different regions of Melanesia (Papua New Guinea, Vanuatu, and the Solomon Islands) and Southeast Asia (Thailand and Cambodia). Nearly all isolates (92%) in Melanesia were shown to carry a *dhfr* double mutation (CNRNI [underlining indicates the mutation]) at positions 50, 51, 59, 108, and 164, whereas 98% of Southeast Asian isolates were either triple (CIRNI) or quadruple (CIRNL) mutants. Microsatellite analysis revealed two distinct lineages of *dhfr* double mutants in Melanesia. One lineage had the same microsatellite haplotype as that previously reported for Southeast Asia and Africa, suggesting the spread of this allele to Melanesia from Southeast Asia. The other lineage had a unique, previously undescribed microsatellite haplotype, indicative of the de novo emergence of pyrimethamine resistance in Melanesia.

Malaria is a major cause of morbidity and mortality in large areas of the tropical world. The antifolate drug sulfadoxine-pyrimethamine (SP) has been widely used to treat uncomplicated malaria, mainly as a monotherapy, but also in combination with other antimalarial drugs in most regions of endemicity for malaria in the world.

Pyrimethamine and sulfadoxine inhibit two separate enzymes in the folate synthesis pathway of *Plasmodium falciparum*: dihydrofolate reductase (DHFR) and dihydropteroate synthase (DHPS), respectively. Point mutations at amino acid positions 16, 50, 51, 59, 108, and 164 in the DHFR gene (*dhfr*) are the major causes of resistance to pyrimethamine (3, 17, 18, 24). The mutation at position 108 (Ser→Asn) appears to be an initial prerequisite for a significant (10-fold) increase in in vitro resistance (24). Additional mutations at other amino acid positions within the gene are associated with stepwise increases in resistance. Isolates harboring four mutations at positions 51, 59, 108, and 164 (CIRNL at positions 50, 51, 59, 108, and 164 [mutations are indicated by underlining]) show the highest pyrimethamine resistance so far described.

Various *dhfr* alleles have been observed in regions of endemicity (30). A *dhfr* triple mutant (CIRNI) represents the most common type in Africa and Southeast Asia, while the *dhfr* quadruple mutant (CIRNL) is observed predominantly in Thailand and some other regions in Southeast Asia where SP resistance is very high (1, 12, 30). Two distinct triple *dhfr* mutant genotypes (RICNI and CICNL) are prevalent in South America (2, 18). A five-amino-acid insertion after position 30, termed the Bolivia repeat, is also exclusive to South America, suggesting two unique and different evolutionary origins of pyrimethamine resistance in South America (2).

The migration of drug-resistant alleles can be traced by the analysis of microsatellite markers closely linked to the gene conferring resistance. Microsatellite analysis flanking *pfcrt* has revealed that chloroquine resistance evolved independently in at least four different regions: Southeast Asia, two regions in South America, and New Guinea (31). Meanwhile, all *dhfr* triple (CIRNI) and quadruple (CIRNL) mutants from Southeast countries displayed the same or nearly identical microsatellite haplotypes flanking *dhfr* (12). Strikingly, pyrimethamine-resistant isolates in Africa also harbored microsatellite haplotypes identical to those found in Southeast Asia (21), suggesting a single origin of pyrimethamine resistance in Southeast Asia, which subsequently spread to Africa. However, whether the Melanesian *dhfr* mutants originated in Southeast Asia or arose independently remains unclear.

In the present study, we determined *dhfr* and microsatellite haplotypes flanking the gene in *P. falciparum* isolates from Melanesia (Papua New Guinea, Vanuatu, and the Solomon Islands) and Southeast Asia (Thailand and Cambodia). Our

* Corresponding author. Mailing address: Department of International Affairs and Tropical Medicine, Tokyo Women's Medical University School of Medicine, 9-1 Kawada-cho, Shinjuku-ku, Tokyo 162-8666, Japan. Phone: 81 3 5269 7422. Fax: 81 3 5269 7422. E-mail: hiro-tm@research.twmu.ac.jp.

▽ Published ahead of print on 8 January 2007.

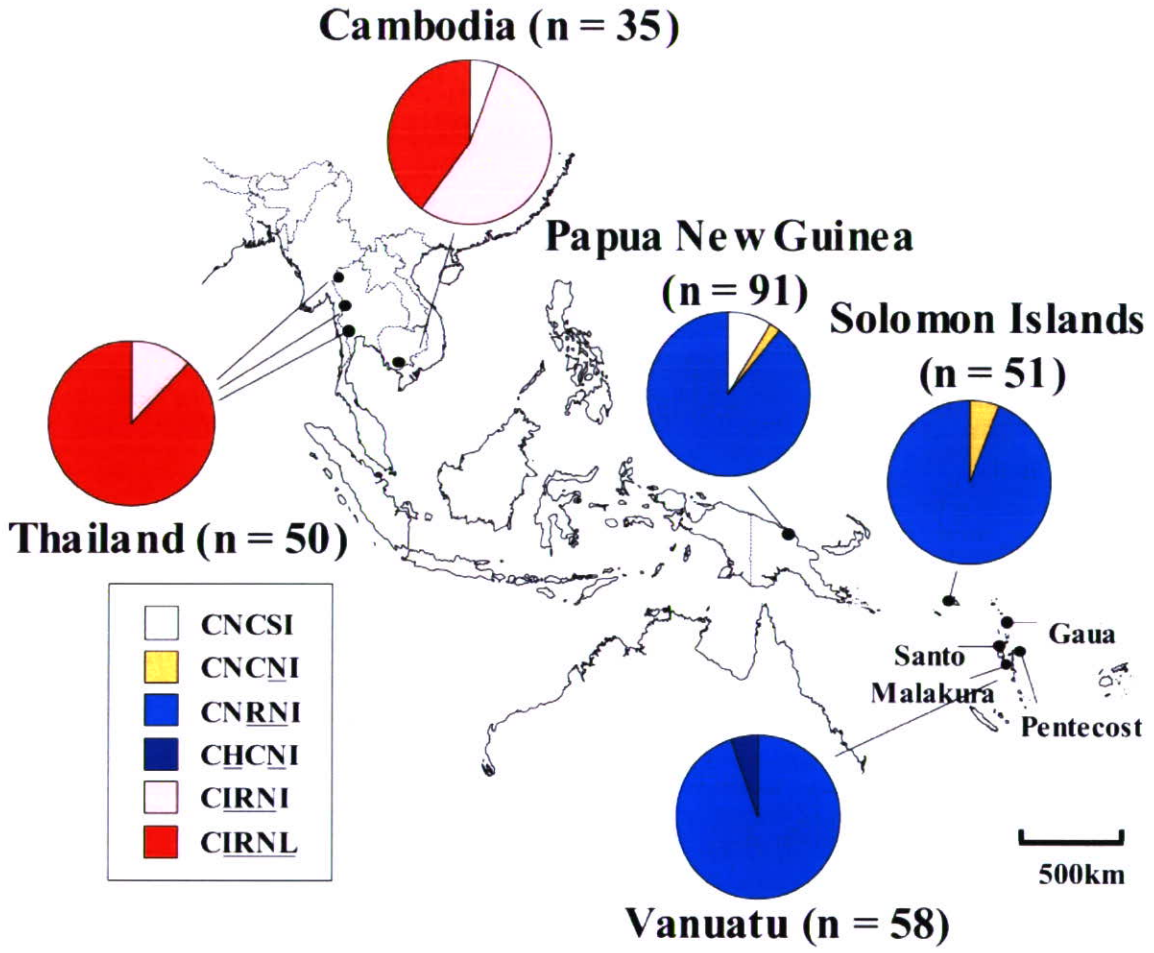

FIG. 1. Frequency of *dhfr* genotypes in *P. falciparum* isolates from Papua New Guinea, the Solomon Islands, Vanuatu, Cambodia, and Thailand.

results show two major lineages of pyrimethamine resistance in Melanesia. One has apparently originated in Melanesia, while the other originated in Southeast Asia and spread to Africa and Melanesia. This is the first unambiguous demonstration of the unique evolution of *P. falciparum* pyrimethamine resistance in Melanesia.

MATERIALS AND METHODS

Study site and patients. Blood samples were obtained from *P. falciparum*-infected patients living in five countries where malaria is endemic: (i) Papua New Guinea, where isolates were from finger-prick blood samples taken during in vitro studies at a town clinic in Wewak, East Sepik Province, in November of both 2002 and 2003 (9, 10); (ii) Solomon Islands, where isolates from venous-blood samples were taken as part of a cross-sectional survey of three villages located in the northwestern part of Guadalcanal in 1995 and 1996 (23); (iii) Vanuatu, where isolates were from finger-prick blood samples obtained during a cross-sectional survey of rural villages and primary schools from February to March 1996 to 1998 in four islands, Gaua, Santo, Pentecost, and Malakula (22); (iv) Cambodia, where isolates were obtained from finger-prick blood samples taken during a cross-sectional survey of rural villages in Chumkiri, Kampot Province, in December 2004; (v) Thailand, where isolates were obtained from pretreatment venous blood samples taken during in vitro studies at a town clinic located at the western border of Tak, Kanchanaburi and Ratchaburi provinces, from 2001 to 2002.

DNA preparation. Finger-prick blood (75 μl) was spotted onto chromatography filter paper ET31CHR (Whatman Limited, Kent, United Kingdom). Venous blood was transferred into heparin-containing test tubes. Parasite DNA was purified using a QIAamp DNA blood mini kit (QIAGEN, Germany) according to the manufacturer's instructions with some modifications (22).

***dhfr* genotyping.** *dhfr* was amplified by PCR, and amplified products were directly sequenced with a BigDye Terminator 1.1 cycle sequencing kit in the ABI 377 DNA sequencer (GE Healthcare UK Ltd., Buckinghamshire, England) as previously reported (10, 19).

Microsatellite haplotyping. In order to determine the evolutionary history of pyrimethamine-resistant alleles of *dhfr*, we measured variation in the number of TA repeats at six microsatellite loci closely linked to the gene. These were located on chromosome 4, 0.1, 3.87, and 4.49 kb upstream and 0.52, 1.48, and 5.87 kb downstream of *dhfr*. In some cases, in order to estimate the limit of genetic hitchhiking, which is defined as a valley of reduced variation around *dhfr*, an additional six-microsatellite markers were analyzed at 7.55, 29.61, 57.68, and 363.33 kb upstream and 30.31 and 299.72 kb downstream of *dhfr*. Polymorphisms in these microsatellite markers were determined as previously described (12). Briefly, seminested PCR was performed using fluorescent end-labeled primers. Size variations in the amplified products were determined by electrophoresis on an ABI 377 sequencer and analyzed with GeneScan software (GE Healthcare UK Ltd.). Samples with two or more peaks at the same locus in the electropherogram were considered to be mixed infections and were excluded from further analysis.

Polymorphism between microsatellite markers is measured as variation in nucleotide length derived from various numbers of TA repeats. Microsatellite haplotypes harboring an association of bp 200-194-176-106-203-111 at microsatellite positions 4.49, 3.87, and 0.1 kb upstream and 0.52, 1.48, and 5.87 kb downstream of *dhfr* were designated "SEA" haplotypes, and those harboring an association of bp 220-202-156-100-205-111 were designated "Melanesia" haplotypes. Microsatellite haplotypes showing slight differences at one or two microsatellite markers from the SEA haplotype, e.g., at bp 204- 200-176-106-203-111

TABLE 1. Microsatellite polymorphisms in 15 *P. falciparum* isolates with wild-type *dhfr* or single-mutant *dhfr*

Isolate	Country[a]	Size (bp) of microsatellite marker at indicated position (kb)					
		−4.49	−3.87	−0.1	+0.52	+1.48	+5.87
CNCSI	Cambodia	198	206	156	94	203	105
(*n* = 10)	Cambodia	198	206	156	94	203	105
	PNG	202	196	156	94	203	121
	PNG	214	198	156	94	203	123
	PNG	202	192	156	96	203	115
	PNG	204	194	172	96	203	103
	PNG	204	194	172	92	203	103
	PNG	204	206	172	100	203	111
	PNG	202	192	176	96	203	115
	PNG	202	192	176	96	203	115
CNCNI	Solomon	210	194	172	96	203	113
(*n* = 5)	Solomon	204	208	176	94	203	120
	Solomon	204	208	176	94	203	120
	PNG	210	194	178	102	203	113
	PNG	210	194	178	102	203	113

[a] PNG, Papua New Guinea; Solomon, Solomon Islands.

(underlining indicates the differences), were considered SEA variation haplotypes. Similarly, haplotypes displaying minor variation at one or two markers from the Melanesia haplotype, e.g., bp 220-202-156-100-205-113, were considered Melanesia variation haplotypes. Isolates showing mixed *dhfr* genotypes and/or microsatellite haplotypes were excluded from analysis.

Statistical analysis. We calculated the expected heterozygosity (h) at each microsatellite locus as $h = [n/(n-1)][1 - \Sigma p_i^2]$, where n is the number of infections sampled and p_i^2 is the frequency of the i^{th} allele. The sampling variance of h was calculated according to the following formula (23), a slight modification of the standard diploid variance (13), $[2/n(n-1)]\{2(n-2)[\Sigma pi^3 - (\Sigma pi^2)^2] + \Sigma pi^2 - (\Sigma pi^2)^2\}$. A P value of <0.05 was considered statistically significant.

Nucleotide sequence accession number. The complete sequence of the allele identified has been submitted to the DDBJ and assigned accession number AB271908.

RESULTS

***dhfr* genotypes.** Among a total of 314 samples, 29 (9%) had multiple *dhfr* alleles and/or were of mixed microsatellite haplotypes and so were excluded from this analysis. *dhfr* allele types and flanking microsatellite haplotypes were thus determined for 285 isolates (91 from Papua New Guinea, 51 from the Solomon Islands, 58 from Vanuatu, 35 from Cambodia, and 50 from Thailand). The frequencies of *dhfr* genotypes differed considerably between Southeast Asia and Melanesia (Fig. 1). In Southeast Asia, nearly all parasites (98%) carried either triple (CIRNI at positions 50, 51, 59, 108, and 164) or quadruple (CIRNL) mutations at *dhfr*. In Cambodia, triple and quadruple mutants were near equally prevalent. In Thailand, 85% of isolates were quadruple mutants. In Melanesia, nearly all isolates (92%) harbored a *dhfr* double mutation (CNRNI). The pyrimethamine-sensitive, wild-type allele (CNCSI) was found in only Papua New Guinea and at relatively low prevalence (8%). Neither the triple (CIRNI) nor the quadruple (CIRNL) mutant was found in Melanesia. A unique CHCNI allele was observed in three isolates from Gaua Island, Vanuatu.

Polymorphism in microsatellite markers flanking *dhfr*. The polymorphisms in six microsatellite markers flanking *dhfr* (−4.49 to 5.87 kb) from wild-type (n = 10) or single-mutant (n = 5) isolates are shown in Table 1. For those parasites carrying pyrimethamine-sensitive, wild-type alleles of *dhfr*, microsatellite markers were highly polymorphic. In contrast, *dhfr* double-mutant isolates (n = 184) showed remarkably little diversity at all loci (Fig. 2). Similarly, nearly all triple (n = 25) and quadruple (n = 58) mutants displayed limited microsatellite polymorphism at each locus (Fig. 2). The expected heterozygosity (h) at each microsatellite marker is given in Table 2. In isolates carrying wild-type or single-mutant *dhfr* alleles, h was high (0.60 to 0.89) at all six loci located between 4.49 kb upstream and 5.87 kb down-

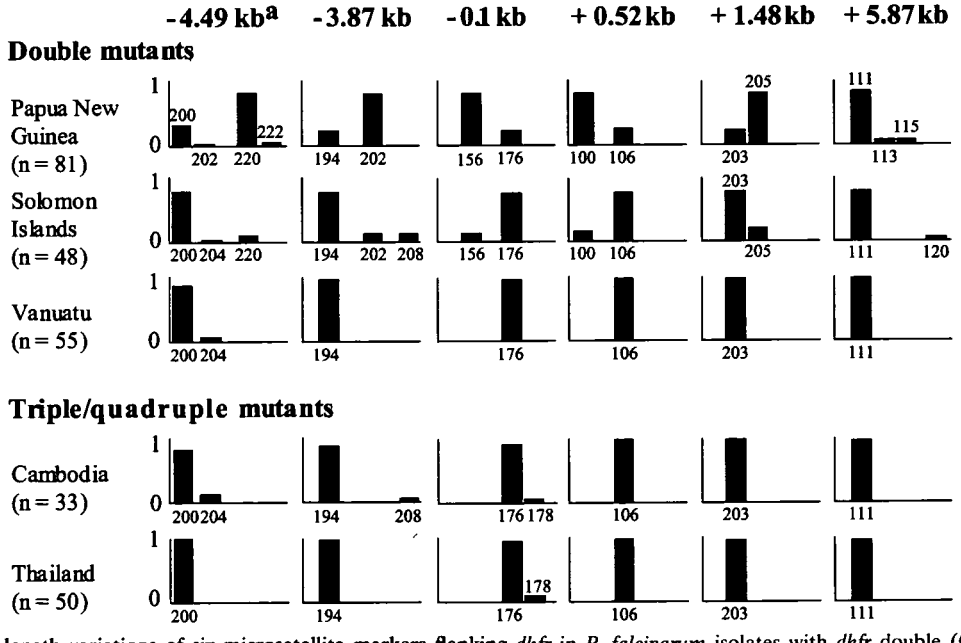

FIG. 2. Repeat length variations of six microsatellite markers flanking *dhfr* in *P. falciparum* isolates with *dhfr* double (CNRNI) and triple (CIRNI)/quadruple (CIRNL) mutants. x axes, size (bp) of microsatellite markers. y axes, frequency of microsatellite alleles. [a], location of microsatellite marker (distance from *dhfr*).

TABLE 2. Expected heterozygosity of microsatellite markers in *P. falciparum* isolates

Isolate	No. of isolates	*h* of microsatellite marker at indicated position (kb)						No. of haplotypes
		−4.49	−3.87	−0.1	+0.52	+1.48	+5.87	
CNCSI	10	0.78	0.84	0.69	0.71	0	0.89	8
CNCNI	5	0.60	0.60	0.80	0.80	0	0.60	5
CNRNI	184	0.54	0.49	0.48	0.49	0.48	0.17	2[a]
CIRNI	25	0.28	0.22	0.08	0	0	0	1[a]
CIRNL	58	0	0	0.10	0	0	0	1[a]

[a] Number of major haplotypes.

stream of *dhfr*, except at the monomorphic +1.48-kb locus. In contrast, those isolates carrying the triple or quadruple mutations at *dhfr* had very low *h* values (0 to 0.28) at all microsatellite loci, indicating limited diversity in those isolates. Isolates carrying double mutations at *dhfr* had intermediate values of *h* (0.48 to 0.54) lying somewhere between those of the wild-type/single mutants and triple/quadruple mutants.

Microsatellite haplotypes. Different microsatellite haplotypes were found in isolates carrying wild-type *dhfr* and in those carrying single mutations; 8 haplotypes were found in 10 wild-type *dhfr* isolates, and 3 haplotypes were found in 5 single mutants (Table 1). In contrast, only two distinct microsatellite haplotypes (SEA/SEA variation and Melanesia/Melanesia variation) were observed in a total of 184 *dhfr* double-mutant isolates (Fig. 3). Identical or very similar haplotypes (SEA/SEA variation) were found in all *dhfr* triple or quadruple mutation-carrying isolates (n = 83), suggesting that *dhfr* triple and quadruple mutants evolved directly from the *dhfr* double mutant.

In Southeast Asia, only SEA/SEA variation haplotypes were observed. These haplotypes were also predominant in Melanesian countries, except Papua New Guinea, where 78% of isolates were of the Melanesia/Melanesia variation haplotypes. In Vanuatu, all isolates showed SEA/SEA variation haplotypes. One isolate carrying a hybrid of the SEA and Melanesia haplotypes (it was of SEA haplotype upstream and Melanesia haplotype downstream of *dhfr*, bp 200-194-176-100-205-111) was observed in the Solomon Islands.

Genetic hitchhiking in *dhfr* double-mutant parasites from Papua New Guinea. These results suggest that the *dhfr* double mutants present today in Melanesia emerged independently in Southeast Asia and Melanesia. To determine the history of these two lineages, we measured the extent of genetic hitchhiking, which is determined by the distance of reduced microsatellite variation around *dhfr*. For this purpose, the variance

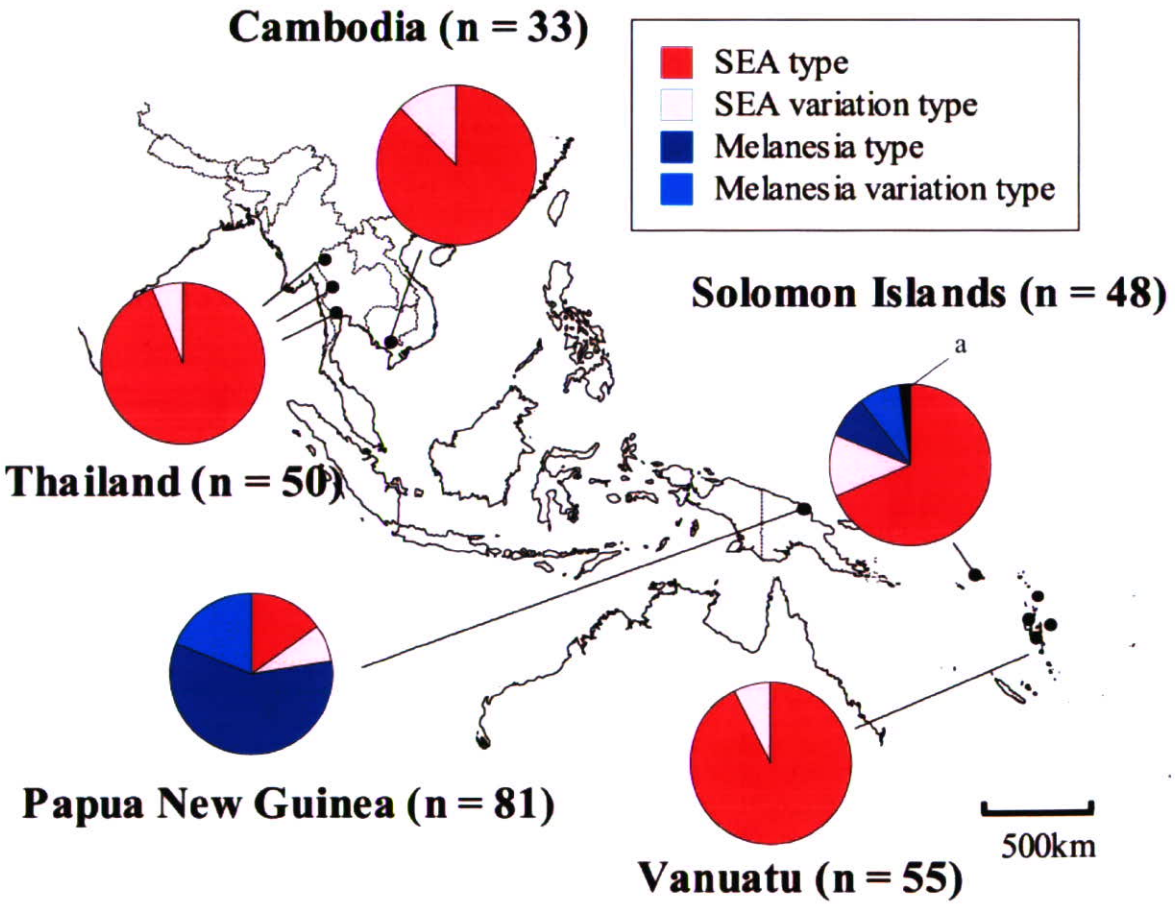

FIG. 3. Frequency of microsatellite haplotype flanking *dhfr* in *P. falciparum* isolates with *dhfr* double, triple, or quadruple mutants from Papua New Guinea, the Solomon Islands, Vanuatu, Cambodia, and Thailand. [a], isolate (n = 1) carrying a hybrid of the SEA and Melanesia haplotypes (it was of SEA haplotype upstream and Melanesia haplotype downstream of *dhfr*, bp 200-194-176-100-205-111).

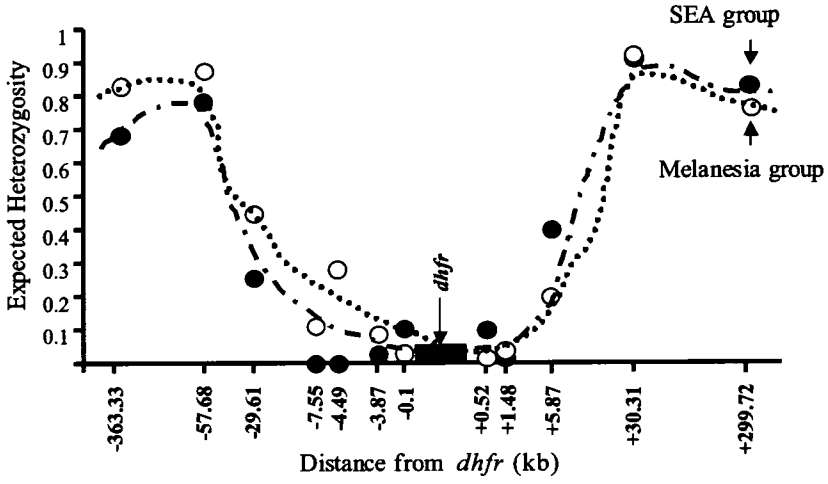

FIG. 4. Reduced microsatellite polymorphism near *dhfr* in *P. falciparum* isolates with CNRNI genotype from Papua New Guinea.

of *h* at 12 microsatellite markers spanning 363.33 kb upstream to 299.72 kb downstream of *dhfr* was measured for Papua New Guinean isolates with a *dhfr* double mutant displaying a SEA/SEA variation haplotype (n = 17) and those displaying the Melanesia/Melanesia variation haplotype (n = 64) (Fig. 4). The patterns of genetic hitchhiking in both haplotypes were similar within a distance of 58 kb upstream and 30 kb downstream of *dhfr*. These results suggest that these two lineages, both carrying the same point mutations (CNRNI), appeared coincidentally in Papua New Guinea.

DISCUSSION

This study clearly shows that pyrimethamine-resistant *P. falciparum* evolved independently in Melanesia. It has previously been shown that a single lineage of pyrimethamine-resistant parasites arose in Southeast Asia, and subsequently spread to Africa (21). Pyrimethamine-resistant parasites from South America, which show *dhfr* genotypes different from those of other geographic areas, independently evolved in two foci within South America (2). Thus, there are at least four distinct independent origins of *dhfr* resistance presently identified. This is similar to the situation with chloroquine resistance, which has also been reported to have arisen independently a total of four times, once in Southeast Asia, twice in South America, and once in Melanesia (31).

A recent study has reported multiple origins of *dhfr* resistance within Kenya (6). However, care must be taken when basing conclusions about the origins of drug resistance on microsatellite variation from areas of high endemicity, such as Kenya. Two factors are likely to affect microsatellite polymorphism in areas of intense transmission. First, new microsatellite haplotypes are easily generated by meiotic recombination because of a high recombination rate and high prevalence of mixed-haplotype infections. Second, interallelic recombination within a microsatellite may generate new microsatellite alleles by an unequal crossing-over mechanism. Indeed, in a study by Roper et al. (21), nonuniform microsatellite haplotypes were noticeable around *dhfr* in pyrimethamine-resistant African isolates. These factors may be less important in areas of low transmission, such as Southeast Asia, and so do not compromise the conclusions of the present study.

Genetic hitchhiking reduces the expected heterozygosity of microsatellite markers around a selected gene, resulting in a valley of reduced variation. However, this association is easily broken down by recombination, resulting in a narrowing of the selection valley as the number of generations increases. In this study, we compared the selection valleys around the *dhfr* gene in two *dhfr* double mutants carrying SEA and Melanesia microsatellite haplotypes from Papua New Guinea. In both haplotypes, the microsatellite patterns within the valley were very similar from a distance of 58 kb upstream to 30 kb downstream of *dhfr*. The size of a selection valley is determined by several different parameters: the strength of the selection pressure on the mutant allele, the frequency of recombination, the transmission intensity, and the number of parasite generations since the emergence of the selected allele (16). In this analysis, these four parameters could be considered equal because all isolates were sampled from the same area. Thus, these results indicate that two ancestors of the *dhfr* double mutant in Papua New Guinea emerged coincidentally: one came from Southeast Asia, and the other arose independently within Melanesia. Although the appearance of the two resistant lineages emerged nearly simultaneously, we consider that the Melanesian-resistant type might have appeared slightly earlier than the influx of the SEA-resistant type. This is because if the SEA-resistant type migrated to Papua New Guinea earlier, it would have swept away microsatellite polymorphisms linked to the wild *dhfr*. Therefore, the possibility that a novel *dhfr*-resistant type having distinct microsatellite haplotypes appeared soon after the sweep in Papua New Guinea seems very unlikely.

The way drugs are used within regions of endemicity affects the generation and selection of resistant alleles. SP was widely used in Thailand and Cambodia during the 1970s and 1980s as the first-line treatment for uncomplicated malaria. In Melanesian countries, SP was introduced as a first-line treatment during the mid-1990s. Up until this time, pyrimethamine monotherapy was infrequently used for the treatment of malaria and other infections. It is difficult, therefore, to explain the nearly simultaneous emergence of pyrimethamine-resistant parasites